weighing between 2.3 and 4.2 kg were anesthetized with an intraperitoneal injection of pentobarbital sodium (30–35 mg/kg) and ventilated mechanically with room air mixed with oxygen. The depth of anesthesia was maintained with a continuous intravenous infusion of pentobarbital sodium (1–2 mg kg^{-1} h^{-1}) through a catheter inserted into the right femoral vein. Systemic arterial pressure (AP) was monitored from a catheter inserted into the right femoral artery. The heart rate (HR) was determined from an electrocardiogram using a cardiotachometer. The esophageal temperature of the animal was measured using a thermometer (CTM-303, TERUMO, Japan) and was maintained at approximately 37 °C using a heated pad and a lamp.

Bilateral vagal nerves were exposed and sectioned through a midline cervical incision. With the animal in the lateral position, the left fifth and sixth ribs were resected to allow access to the heart. The heart was suspended in a pericardial cradle. Using a fine guiding needle, a dialysis probe was implanted into the anterolateral free wall of the left ventricle perfused by the left anterior descending coronary artery (LAD) (Akiyama et al., 1994). A 3-0 silk suture was passed around the LAD just distal to the first diagonal branch for subsequent coronary occlusion. For bilateral vagal stimulation, a pair of bipolar platinum electrodes was attached to the cardiac end of each sectioned vagal nerve. The nerves and electrodes were covered with warmed mineral oil for insulation. Heparin sodium (100 U/kg) was administered intravenously to prevent blood coagulation. At the end of the experiment, the animals were killed with an overdose of intravenous pentobarbital sodium. We confirmed that the semipermeable membrane of the dialysis probe had been implanted within the left ventricular myocardium.

Dialysis technique

The materials and properties of the transverse dialysis probe have been previously described (Kitagawa et al., 2005). Briefly, both ends of a dialysis fiber (length, 8 mm; outer diameter, 215 μm; inner diameter, 175 μm; pore size, 300 Å; Evaflux type 5A, Kuraray Medical, Japan) were glued to polyethylene tubes (length, 25 cm; outer diameter, 500 μm; inner diameter, 200 μm). The dialysis probe was perfused with Ringer's solution at the rate of 5 μl/min using a microinfusion pump (CMA/100, Carnegie Medicine). Dialysate sampling was initiated 2 h after implanting the dialysis probe, at which point the concentration of myoglobin in the dialysate had reached a steady state (Kitagawa et al., 2005). The actual dialysate sampling period lagged behind a given collection period by 2 min due to the dead space volume between the dialysis membrane and the sample tube. The concentration of myoglobin in the dialysate was measured immunochemically (Cardiac Reader, Roche Diagnostics). The detection limit for myoglobin was 30 ng/ml. The sample was diluted in Ringer's solution whenever necessary and the concentration was corrected for the dilution factor.

Protocols

Protocol 1 (VX group, n=6)

As a control group, we measured changes in the myocardial interstitial myoglobin levels of vagotomized cats subjected to 60 min of LAD occlusion followed by 60 min of reperfusion. After collecting a 15-min baseline dialysate sample, we occluded the LAD for 60 min and collected four consecutive 15-min dialysate samples during the ischemic period. We then released the occlusion and collected additional four consecutive 15-min dialysate samples during the 60-min reperfusion period.

Protocol 2 (VS group, n=6)

We examined the effects of bilateral vagal stimulation on the release of myocardial interstitial myoglobin. To avoid the potential preconditioning mimetic effects of ACh released in response to the vagal stimulation (Kawada et al., 2002; Przyklenk and Kloner, 1995), we initiated bilateral vagal stimulation (5 Hz, 10 V, 1-ms pulse duration) immediately after the LAD occlusion and continued it throughout the 60-min ischemic period and the 60-min reperfusion period. Dialysate samples were collected in the same manner described for Protocol 1.

Protocol 3 (VS-W group, n=6)

Because PI3K is involved in the direct cardioprotective effects of ACh (Qin et al., 2003; Oldenburg et al., 2003), we examined the contribution of PI3K to the effects of vagal stimulation on ischemia-induced myocardial injury. A PI3K inhibitor wortmannin was administered (0.6 mg/kg i.v. bolus) 15 min before the onset of the baseline dialysate sampling. After collecting the baseline dialysate sample, LAD occlusion and reperfusion were each performed for 60 min. Bilateral vagal stimulation was started immediately after the LAD occlusion and was continued until the end of the reperfusion period. Dialysate samples were collected as described in Protocol 1.

Protocol 4 (VS-P group, n=6)

Because bradycardia is a major hemodynamic change induced by vagal stimulation, we examined the contribution of bradycardia to the effects of vagal stimulation on ischemia-induced myocardial injury. After collecting the baseline dialysate sample, LAD occlusion and reperfusion were each performed for 60 min. Bilateral vagal stimulation and fixed-rate ventricular pacing (200 beats/min) were both started immediately after the LAD occlusion and were continued throughout the ischemic and reperfusion periods. Dialysate samples were collected as described in Protocol 1.

Statistical analysis

All data are presented as the means and SE. To examine the effects of coronary occlusion and reperfusion on the myocardial interstitial myoglobin levels in each group, we compared the myoglobin levels during the ischemic and reperfusion periods with the baseline level (eight comparisons) and the myoglobin levels during the reperfusion period with the myoglobin level during the last 15 min of ischemia (four comparisons) using Holm's t test for 12 comparisons (Glantz, 2002). Briefly, after calculating P values for the 12 comparisons using paired-t test, the P values were sorted based on their size. The smallest P value was multiplied by 12 (the number of total comparisons), the next smallest P value was multiplied by 11 (the number of total comparisons minus 1), and so on. The Holm's test is less conservative than the ordinary Bonferroni method. Because the myoglobin level changed by more than an order of magnitude, comparisons were made after a logarithmic conversion. Differences were considered significant at $P<0.05$.

To compare myoglobin levels among the VX, VS, VS-W and VS-P groups, we used one-way ANOVA (analysis of variance). When there were significant differences among the groups, Dunnett's test was applied to examine the differences between the VS, VS-W, or VS-P group and the VX group (Glantz, 2002). The myoglobin levels at different time points as well as averaged myoglobin levels during the ischemic period, reperfusion period, and total period throughout ischemia and reperfusion were compared. Differences were considered significant at $P<0.05$.

HR and mean AP were measured immediately before the LAD occlusion (denoted as time 0), at 15, 30, 45 and 60 min of ischemia and at 15, 30, 45 and 60 min of reperfusion. The data for the HR and mean AP were compared among the VX, VS, VS-W, and VS-P groups using one-way ANOVA followed by Dunnett's test with the VX group value as the control. Differences were considered significant at $P<0.05$.

Results

Changes in the myocardial interstitial myoglobin levels are summarized in Fig. 1. In the VX group, the LAD occlusion significantly

increased the myoglobin levels compared with the baseline level, suggesting that acute myocardial ischemia disrupted the plasma membrane of the myocardium, allowing myoglobin to leak into the myocardial interstitium. The myoglobin level during the last 15 min of ischemia reached, on average, 12 times the baseline myoglobin level. Reperfusion further increased the myoglobin level. The myoglobin level during the first 15 min of reperfusion was, on average, three times higher than the myoglobin level during the last 15 min of ischemia. After 15 min of reperfusion, the myoglobin level declined gradually with time but remained higher than the baseline level until the last 15 min of the reperfusion period. In the VS group, the time course was similar but the changes in the myoglobin levels during the ischemia and reperfusion periods were smaller than those observed in the VX group. In the VS-W group, changes in the myoglobin levels were attenuated compared to those observed in the VX group and no significant increase in myoglobin was detected upon reperfusion. In the VS-P group, changes in the myoglobin levels showed intermediate values, which were between those observed in the VX and VS groups.

Baseline myoglobin levels were not significantly different among the VX, VS, VS-W, and VS-P groups (157±40, 110±23, 124±48, and 118±30 ng/ml, respectively). Average myoglobin levels for the ischemic period (Fig. 2A), reperfusion period (Fig. 2B), and total period (Fig. 2C) were significantly lower in the VS and VS-W groups compared with the VX group.

Changes in HR are summarized in the top panel of Fig. 3. Baseline HR did not markedly differ among the four groups. In the VS group (filled circles), vagal stimulation decreased the HR throughout the ischemic and reperfusion periods compared with the HR in the VX group (open circles). After the cessation of vagal stimulation (denoted as "vagal stim off"), the HR in the VS group returned toward the baseline level. In the VS-W group (double circles), vagal stimulation decreased the HR at 15 and 30 min compared with the results from the VX group. Although the HR from 45 to 120 min did not differ significantly compared with the VX group, the cessation of vagal stimulation increased the HR, suggesting that vagal stimulation was effective until the end of the reperfusion period. In the VS-P group (open squares), the HR was maintained at 200 beats/min using ventricular pacing. The cessation of ventricular pacing (denoted as "pacing off") significantly decreased the HR below the baseline level, suggesting that vagal stimulation was effective during the ventricular pacing.

Changes in AP are summarized in the bottom panel of Fig. 3. Differences in AP between the VS and VX groups were not statistically significant. Although pretreatment with wortmannin increased the AP in the VS-W group, differences in AP between the VS-W and VX groups were not statistically significant at any time point. In the VS-P group, AP at 15 min was significantly lower compared with that in the VX group.

Discussion

Vagal stimulation-induced cardioprotection against ischemic injury

Cardiac microdialysis is a useful method to monitor changes in myocardial interstitial myoglobin levels in an ischemic region (Kitagawa et al., 2005). LAD occlusion increased the myoglobin level in the myocardial interstitium in the VX group (Fig. 1). Vagal stimulation, initiated immediately after the LAD occlusion, suppressed myoglobin release during ischemia (Figs. 1 and 2A). In addition to preventing lethal ventricular arrhythmia during acute myocardial ischemia (Myers et al., 1974; Rosenshtraukh et al., 1994; Vanoli et al., 1991), vagal stimulation also appears to reduce myocardial damage in the ischemic region. Because we avoided large ischemia by occluding LAD just distal to the first diagonal branch, lethal ventricular

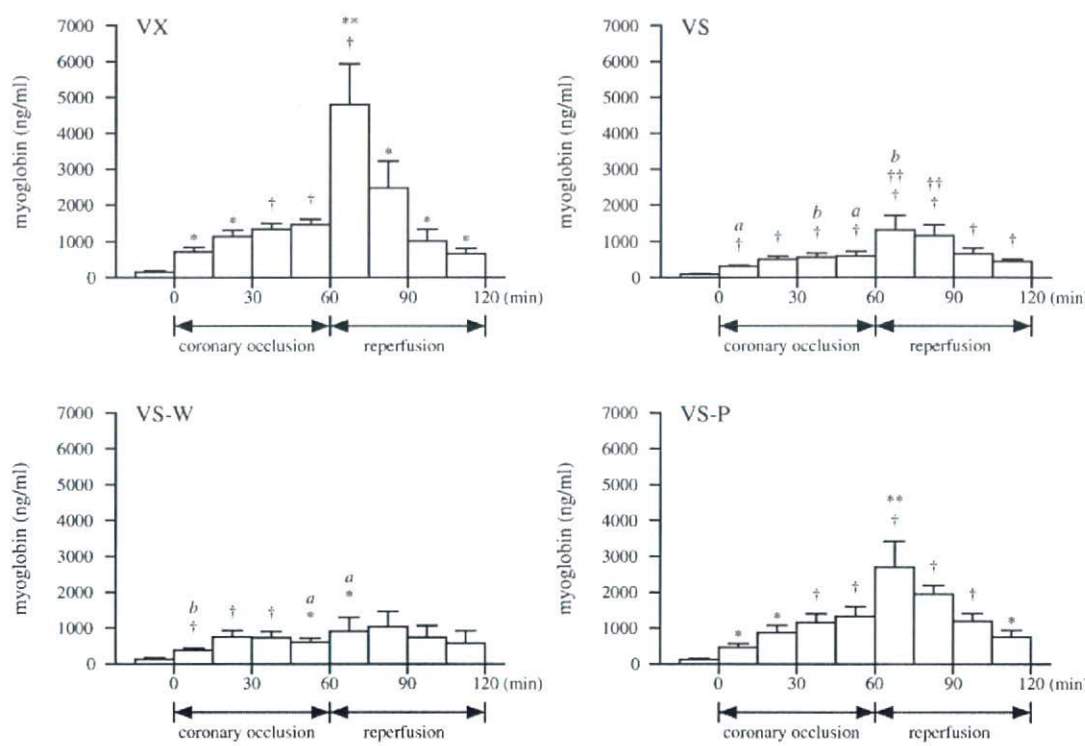

Fig. 1. Changes in the myocardial interstitial myoglobin levels in the VX, VS, VS-W, and VS-P groups. After collecting baseline dialysate samples, the left anterior descending coronary artery was occluded for 60 min and then reperfused for 60 min. Acute myocardial ischemia significantly increased the myoglobin level in the ischemic region. Reperfusion further increased the myoglobin level. Data are shown as the means+SE ($n=6$ each). †$P<0.01$ and *$P<0.05$ compared with the baseline value. ††$P<0.01$ and **$P<0.05$ compared with the myoglobin level during the last 15 min of ischemia. $^{a}P<0.01$ and $^{b}P<0.05$ compared with the corresponding myoglobin level in the VX group.

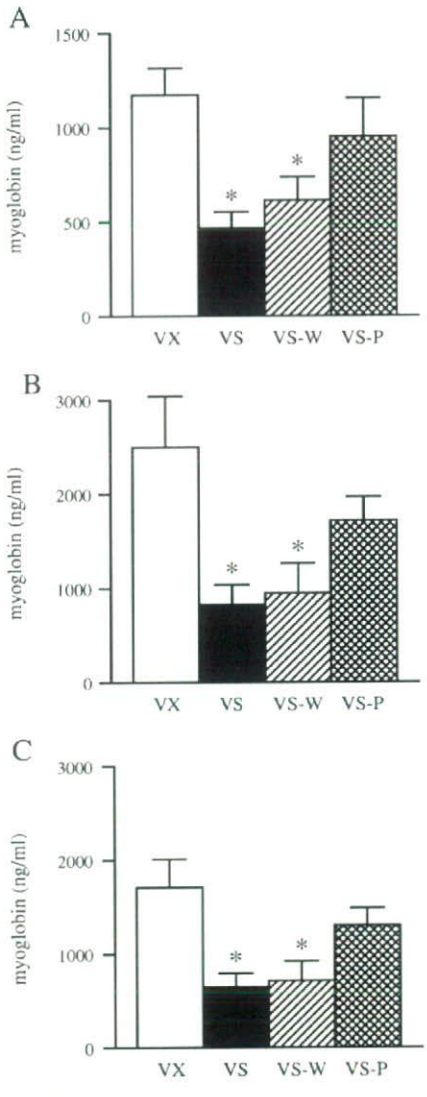

Fig. 2. Average myoglobin levels for the ischemic period (A), reperfusion period (B), and total period throughout ischemia and reperfusion (C). In all panels, the myoglobin levels were significantly lower in the vagal stimulation (VS) and vagal stimulation with wortmannin pretreatment (VS-W) groups than in the control, vagotomized (VX) group. The myoglobin levels in the vagal stimulation with fixed-rate pacing (VS-P) group did not markedly differ from those in the VX group. Data are shown as the means + SE ($n = 6$ each). *$P < 0.05$ compared with the VX group.

arrhythmia scarcely occurred in the present experimental settings. The cardioprotective effect induced by vagal stimulation may include direct effects of ACh on the ischemic myocardium and indirect effects induced through altered hemodynamics.

For the direct effects, ACh administered prior to a coronary artery occlusion can exert a preconditioning mimetic effect via a signaling pathway that includes PI3K (Qin et al., 2003; Oldenburg et al., 2003). Because we initiated vagal stimulation immediately after the LAD occlusion, however, the mechanism underlying the reduced myocardial damage observed in the present study is likely independent of the preconditioning mimetic effect. In support of this interpretation, the inhibition of PI3K did not affect the reduced myoglobin release induced by vagal stimulation (Fig. 2A, VS-W group). The results of the present study, however, did not preclude the direct involvement of ACh through mechanisms other than the PI3K pathway.

For the indirect effects, bradycardia reduces myocardial oxygen consumption by decreasing the number of ventricular contractions per unit time (Sammel et al., 1983; Shinke et al., 1999). Vagal stimulation also dilates normal coronary arteries via ACh and vasoactive intestinal polypeptide release (Feigl, 1969; Reid et al., 1985; Feliciano and Henning, 1998; Henning and Sawmiller, 2001), which may increase collateral flow into the ischemic region. Bradycardia associated with vagal stimulation may increase coronary perfusion due to a prolonged diastolic interval (Buck et al., 1981), reduced ventricular contractility via a force-frequency mechanism (Maughan et al., 1985), and antagonism of the sympathetic effect (Nakayama et al., 2001). These processes may have improved the balance between energy supply and demand, leading to reduced myocardial injury in the ischemic region. In the present study, the VS-P group showed myoglobin levels that were between those of the VX and VS groups (Fig. 2A), suggesting that bradycardia plays a significant role in vagally induced cardioprotection. The observed effect of fixed-rate ventricular pacing on the vagal effect agrees with our previous study (Kawada et al., 2006), in which prevention of bradycardia using ventricular pacing abolished the suppressive effect of vagal stimulation on the ischemia-induced increase in myocardial interstitial norepinephrine levels.

Reperfusion-induced myocardial injury

Reperfusion of the LAD increased the myocardial interstitial myoglobin level compared with that detected during the last 15 min of ischemia (Fig. 1), which agreed with in vivo observations in the rabbit heart (Kitagawa et al., 2005). In the isolated perfused rat heart, 30 min of hypoxia or anoxia increased the concentration of creatinine kinase in the interstitial transudate, an effect that was further augmented by reoxygenation (Wienen and Kammermeier, 1988). The increased levels of these macromolecules upon reperfusion may have resulted from a reperfusion injury. During ischemia, ATP deficiency impairs the operation of Na^+/K^+ ATPases, resulting in the accumulation of intracellular Na^+. Ischemia also causes acidosis in the ischemic region. Upon reperfusion, washing out the excess extracellular H^+ promotes intracellular Na^+ accumulation via Na^+/H^+ exchange. Eventually, Ca^{2+} influx occurs due to reverse-mode operation of Na^+/Ca^{2+} exchangers (Lazdunski et al., 1985). Once the intracellular Ca^{2+} concentration reaches a threshold level, ATP resynthesis causes hypercontracture of myofibrils and cytoskeletal lesions (Piper, 1989; Piper et al., 2004). Additionally, the recovery of myocardial contraction upon reperfusion increases the leakage of

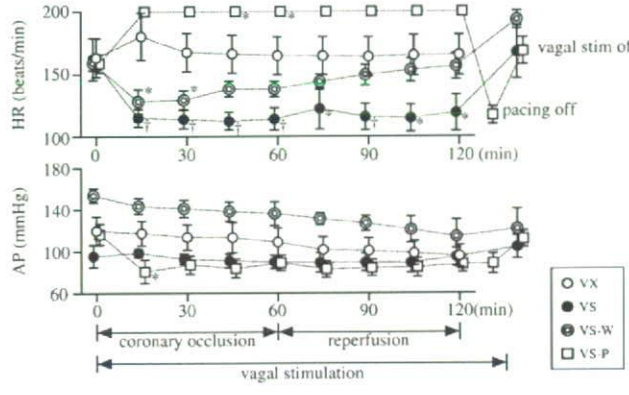

Fig. 3. Changes in heart rate (HR) and arterial pressure (AP). The HR and AP data immediately before the coronary occlusion are shown at time 0. In the vagal stimulation (VX) and vagal stimulation with wortmannin pretreatment (VS-W) groups, cessation of vagal stimulation increased the HR, suggesting that vagal stimulation was effective until the end of the reperfusion period. In the vagal stimulation with fixed-rate pacing group (VS-P), cessation of pacing decreased the HR, whereas cessation of vagal stimulation increased the HR, suggesting that vagal stimulation was effective during ventricular pacing. Data are shown as the means ± SE ($n = 6$ each). †$P < 0.01$ and *$P < 0.05$ compared with the corresponding data from the VX group.

cytosolic molecules from damaged sarcolemmal membranes. For example, ventricular wall stress increases the leakage of lactate dehydrogenase after anoxia in K^+-arrested, isolated, perfused rat heart (Takami et al., 1990). These two explanations are not mutually exclusive and both may contribute to the increased myocardial interstitial myoglobin levels during reperfusion.

In the present study, vagal stimulation significantly reduced the myoglobin levels in the VS and VS-W groups during the reperfusion period (Fig. 2B). The reduced myoglobin levels during the reperfusion period correlated with the decreased myoglobin levels during the ischemic period. It is likely that reduced myocardial injury during the ischemic period contributed to the inhibition of myocardial injury during the reperfusion period. Further studies that include stimulating the vagal nerve during the ischemic or reperfusion period separately may be required to identify the respective effects of vagal stimulation during each of these potentially deleterious events. Although the PI3K signaling pathway played a significant role in the prevention of reperfusion injury by low-pressure reperfusion and postconditioning in the isolated rat heart (Bopassa et al., 2006), the inhibition of PI3K by wortmannin did not antagonize the reduction in myoglobin release induced by vagal stimulation in the present study. The fact that wortmannin inhibits superoxide release from polymorphonuclear leukocytes and exerts cardioprotective effects during myocardial ischemia and reperfusion (Young et al., 2000) makes it difficult to interpret the in vivo effects of wortmannin in blood perfused hearts.

Reperfusion is a pre-requisite to salvaging viable myocardium, following an acute myocardial infarction (Hausenloy and Yellon, 2004). Possible clinical relevance of vagal stimulation is that vagal stimulation may be able to reduce myocardial damage associated with the reperfusion therapy. Endovascular approach (Nabutovsky et al., 2007) may be feasible for vagal stimulation in acute clinical settings. In a long-term treatment, we have shown that intermittent vagal stimulation improves the survival of chronic heart failure following myocardial infarction in rats (Li et al., 2004). On the other hand, bradycardic therapy using a sinus node inhibitor cilobradine also improves left ventricular function and remodeling of chronic heart failure in dogs (Cheng et al., 2007). Although whether bradycardic therapy is equivalent to vagal stimulation remains a matter of investigation, vagal stimulation may be an additional strategy for treatment of myocardial infarction and chronic heart failure.

Limitations

There are several limitations to the present study. First, we did not quantify the infarct size. Although the measurement of myocardial interstitial myoglobin levels are useful to monitor the time course of myocardial injury development, further studies are required to determine the correlation between the local myoglobin levels and infarct size. Second, HR in the VX group declined to approximately 165 beats/min with time elapsed, resulting in the higher HR in the VS-P group than in the VX group. Although the fixed-rate pacing partially reversed the vagally induced protective effect, slowing the pacing rate might have lowered the myoglobin levels in the VS-P group similar to VS group. Finally, while the inhibition of PI3K signaling pathway by pretreatment of wortmannin did not abolish the vagally induced protective effect, expression and/or activation of PI3K signaling pathway components in the ischemic target tissues was not examined. Further studies focusing on the molecular and cellular basis are required to identify the mechanism(s) by which vagal stimulation attenuates the myocardial injury.

Conclusion

Vagal nerve stimulation, initiated immediately after LAD occlusion, reduced myocardial injury as assessed by myocardial interstitial myoglobin levels. The direct effects of ACh on the ischemic myocardium, at least those associated with the PI3K signaling pathway, were not markedly responsible for the vagal stimulation-mediated cardioprotection observed under our experimental conditions. On the other hand, bradycardia played a significant role in the vagal stimulation-induced cardioprotection against acute myocardial ischemia and reperfusion.

Acknowledgments

This study was supported by a Health and Labor Sciences Research Grant for Research on Advanced Medical Technology, a Health and Labor Sciences Research Grant for Research on Medical Devices for Analyzing, Supporting and Substituting the Function of the Human Body, and a Health and Labor Sciences Research Grant H18-Iryo-Ippan-023 from the Ministry of Health, Labour and Welfare of Japan.

References

Akiyama, T., Yamazaki, T., Ninomiya, I., 1994. In vivo detection of endogenous acetylcholine release in cat ventricles. American Journal of Physiology 266 (3 Pt 2), H854–H860.
Bopassa, J.C., Ferrera, R., Gateau-Roesch, O., Couture-Lepetit, E., Ovize, M., 2006. PI 3-kinase regulates the mitochondrial transition pore in controlled reperfusion and postconditioning. Cardiovascular Research 69 (1), 178–185.
Buck, J.D., Warltier, D.C., Hardman, H.F., Gross, G.J., 1981. Effects of sotalol and vagal stimulation on ischemic myocardial blood flow distribution in the canine heart. The Journal of Pharmacology and Experimental Therapeutics 216 (2), 347–351.
Cheng, Y., George, I., Yi, G.H., Reiken, S., Gu, A., Tao, Y.K., Muraskin, J., Qin, S., He, K.L., Hay, I., Yu, K., Oz, M.C., Burkhoff, D., Holmes, J., Wang, J., 2007. Bradycardic therapy improves left ventricular function and remodeling in dogs with coronary embolization-induced chronic heart failure. The Journal of Pharmacology and Experimental Therapeutics 321 (2), 496–476.
Feigl, E.O., 1969. Parasympathetic control of coronary blood flow in dogs. Circulation Research 25 (5), 509–519.
Feliciano, L., Henning, R.J., 1998. Vagal nerve stimulation releases vasoactive intestinal peptide which significantly increases coronary artery blood flow. Cardiovascular Research 40 (1), 45–55.
Glantz, S.A., 2002. Primer of Biostatistics, 5th ed. McGraw-Hill, New York.
Hausenloy, D.J., Yellon, D.M., 2004. New directions for protecting the heart against ischaemia–reperfusion injury: targeting the reperfusion injury salvage kinase (RISK)-pathway. Cardiovascular Research 61 (3), 448–460.
Henning, R.J., Sawmiller, D.R., 2001. Vasoactive intestinal peptide: cardiovascular effects. Cardiovascular Research 49 (1), 27–37.
Kawada, T., Yamazaki, T., Akiyama, T., Mori, H., Inagaki, M., Shishido, T., Takaki, H., Sugimachi, M., Sunagawa, K., 2002. Effects of brief ischaemia on myocardial acetylcholine and noradrenaline levels in anaesthetized cats. Autonomic Neuroscience: Basic and Clinical 95 (1–2), 37–42.
Kawada, T., Yamazaki, T., Akiyama, T., Li, M., Ariumi, H., Mori, H., Sunagawa, K., Sugimachi, M., 2006. Vagal stimulation suppresses ischemia-induced myocardial interstitial norepinephrine release. Life Sciences 78 (8), 882–887.
Kitagawa, H., Yamazaki, T., Akiyama, T., Sugimachi, M., Sunagawa, K., Mori, H., 2005. Microdialysis separately monitors myocardial interstitial myoglobin during ischemia and reperfusion. American Journal of Physiology. Heart and Circulatory Physiology 289 (2), H924–H930.
Lazdunski, M., Frelin, C., Vigne, P., 1985. The sodium/hydrogen exchange system in cardiac cells: its biochemical and pharmacological properties and its role in regulating internal concentrations of sodium and internal pH. Journal of Molecular and Cellular Cardiology 17 (11), 1029–1042.
Li, M., Zheng, C., Sato, T., Kawada, T., Sugimachi, M., Sunagawa, K., 2004. Vagal nerve stimulation markedly improves long-term survival after chronic heart failure in rats. Circulation 109 (1), 120–124.
Maughan, W.L., Sunagawa, K., Burkhoff, D., Graves Jr., W.L., Hunter, W.C., Sagawa, K., 1985. Effect of heart rate on the canine end-systolic pressure–volume relationship. Circulation 72 (3), 654–659.
Myers, R.W., Pearlman, A.S., Hyman, R.M., Goldstein, R.A., Kent, K.M., Goldstein, R.E., Epstein, S.E., 1974. Beneficial effects of vagal stimulation and bradycardia during experimental acute myocardial ischemia. Circulation 49 (5), 943–947.
Nabutovsky, Y., Florio, J., Morgan, K., Grill, W.M., Farazi, T.G., 2007. Lead design and initial applications of a new lead for long-term endovascular vagal stimulation. Pacing and Clinical Electrophysiology 30 (11), S215–S218.
Nakayama, Y., Miyano, H., Shishido, T., Inagaki, M., Kawada, T., Sugimachi, M., Sunagawa, K., 2001. Heart rate-independent vagal effect on end-systolic elastance of the canine left ventricle under various levels of sympathetic tone. Circulation 104 (19), 2277–2279.
Oldenburg, O., Critz, S.D., Cohen, M.V., Downey, J.M., 2003. Acetylcholine-induced production of reactive oxygen species in adult rabbit ventricular myocytes is dependent on phosphatidylinositol 3- and Src-kinase activation and mitochondrial K_{ATP} channel opening. Journal of Molecular and Cellular Cardiology 35 (6), 653–660.
Piper, H.M., 1989. Energy deficiency, calcium overload or oxidative stress: possible causes of irreversible ischemic myocardial injury. Klinische Wochenschrift 67 (9), 465–476.

Piper, H.M., Abdallah, Y., Schäfer, C., 2004. The first minutes of reperfusion: a window of opportunity for cardioprotection. Cardiovascular Research 61 (3), 365–371.
Przyklenk, K., Kloner, R.A., 1995. Low-dose i.v. acetylcholine acts as a "preconditioning-mimetic" in the canine model. Journal of Cardiac Surgery 10 (4), 389–395.
Qin, Q., Downey, J.M., Cohen, M.V., 2003. Acetylcholine but not adenosine triggers preconditioning through PI3-kinase and a tyrosine kinase. American Journal of Physiology. Heart and Circulatory Physiology 284 (2), H727–H734.
Reid, J.V.O., Ito, B.R., Huang, A.H., Buffington, C.W., Feigl, E.O., 1985. Parasympathetic control of transmural coronary blood flow in dogs. American Journal of Physiology 249 (2 Pt 2), H337–H343.
Rosenshtraukh, L., Danilo Jr., P., Anyukhovsky, E.P., Steinberg, S.F., Rybin, V., Brittain-Valenti, K., Molina-Viamonte, V., Rosen, M.R., 1994. Mechanisms for vagal modulation of ventricular repolarization and of coronary occlusion-induced lethal arrhythmias in cats. Circulation Research 75 (4), 722–732.
Sammel, N.L., Norris, R.M., Hughes, C.F., Johnson, R.N., Ashton, N.G., Elliott, R.L., 1983. Severity of canine myocardial infarcts in relation to indices of oxygen demand: preservation of myocardial creatine kinase activity by vagal stimulation and propranolol. Cardiovascular Research 17 (1), 50–60.
Shinke, T., Takeuchi, M., Takaoka, H., Yokoyama, M., 1999. Beneficial effects of heart rate reduction on cardiac mechanics and energetics in patients with left ventricular dysfunction. Japanese Circulation Journal 63 (12), 957–964.
Takami, H., Matsuda, H., Kuki, S., Nishimura, M., Kawashima, Y., Watari, H., Furuya, E., Tagawa, K., 1990. Leakage of cytoplasmic enzymes from rat heart by the stress of cardiac beating after increase in cell membrane fragility by anoxia. Pflügers Archiv 416 (1–2), 144–150.
Vanoli, E., de Ferrari, G.M., Stramba-Badiale, M., Hull Jr., S.S., Foreman, R.D., Schwartz, P.J., 1991. Vagal stimulation and prevention of sudden death in conscious dogs with a healed myocardial infarction. Circulation Research 68 (5), 1471–1481.
Wienen, W., Kammermeier, H., 1988. Intra- and extracellular markers in interstitial transudate of perfused rat hearts. American Journal of Physiology 254 (4 Pt 2), H785–H794.
Young, L.H., Ikeda, Y., Scalia, R., Lefer, A.M., 2000. Wortmannin, a potent antineutrophil agent, exerts cardioprotective effects in myocardial ischemia/reperfusion. The Journal of Pharmacology and Experimental Therapeutics 295 (1), 37–43.

REGULAR PAPER

J. Physiol. Sci. Vol. 58, No. 6; Dec. 2008; pp. 381–388
Online Oct. 10, 2008; **doi:10.2170/physiolsci.RP011508**

Accentuated Antagonism in Vagal Heart Rate Control Mediated through Muscarinic Potassium Channels

Masaki MIZUNO[1], Atsunori KAMIYA[1], Toru KAWADA[1], Tadayoshi MIYAMOTO[2], Shuji SHIMIZU[1,3], Toshiaki SHISHIDO[1], and Masaru SUGIMACHI[1]

[1]Department of Cardiovascular Dynamics, Advanced Medical Engineering Center, National Cardiovascular Center Research Institute, Osaka, Japan; [2]Department of Physical Therapy, Faculty of Health Sciences, Morinomiya University of Medical Sciences, Osaka, Japan; and [3]Japan Association for the Advancement of Medical Equipment, Tokyo, Japan

Abstract: Although muscarinic K^+ (K_{ACh}) channels contribute to a rapid heart rate (HR) response to vagal stimulation, whether background sympathetic tone affects the HR control via the K_{ACh} channels remains to be elucidated. In seven anesthetized rabbits with sinoaortic denervation and vagotomy, we estimated the dynamic transfer function of the HR response by using random binary vagal stimulation (0–10 Hz). Tertiapin, a selective K_{ACh} channel blocker, decreased the dynamic gain (to 2.3 ± 0.9 beats·min^{-1}·Hz^{-1}, from 4.6 ± 1.1, $P < 0.01$, mean ± SD) and the corner frequency (to 0.05 ± 0.01 Hz, from 0.26 ± 0.04, $P < 0.01$). Under 5 Hz tonic cardiac sympathetic stimulation (CSS), tertiapin decreased the dynamic gain (to 3.6 ± 1.0 beats·min^{-1}·Hz^{-1}, from 7.3 ± 1.1, $P < 0.01$) and the corner frequency (to 0.06 ± 0.02 Hz, from 0.23 ± 0.06, $P < 0.01$). Two-way analysis of variance indicated significant interaction between the tertiapin and CSS effects on the dynamic gain. In contrast, no significant interactions were observed between the tertiapin and CSS effects on the corner frequency and the lag time. In conclusion, although a cyclic AMP-dependent mechanism has been well established, an accentuated antagonism also occurred in the direct effect of ACh via the K_{ACh} channels. The rapidity of the HR response obtained by the K_{ACh} channel pathway was robust during the accentuated antagonism.

Key words: systems analysis, transfer function, muscarinic receptor, sympathovagal interaction, accentuated antagonism, rabbit.

Vagal control of heart rate (HR) is mediated by ACh, which activates M_2 muscarinic receptors and heterotrimeric G_i and/or G_o proteins in cardiac myocytes [1]. The actions of ACh are determined by the G_i protein subunits. The α subunits of the G_i proteins inhibit adenylyl cyclase and decrease HR by counteracting the sympathetic effects [2], whereas $\beta\gamma$ subunits activate inwardly rectifying muscarinic K^+ (K_{ACh}) channels and decrease HR by hyperpolarizing the maximum diastolic potential in the sinus node cells [3–5]. Hereafter in the present paper, we refer to the former action as the indirect action of ACh and the latter action as the direct action of ACh. In a previous paper, we demonstrated that a selective K_{ACh} channel blocker tertiapin decreased and slowed the HR response to dynamic vagal stimulation, suggesting that the K_{ACh} channels contribute to a rapid HR response to vagal stimulation [6]. However, whether background sympathetic tone affects HR control via the K_{ACh} channels remains to be elucidated. Because pathophysiological conditions such as chronic heart failure [7], hypertension [8], and obesity [9] often display increased sympathetic nerve activity, it would be important to quantify the effects of background sympathetic tone on the HR response via the K_{ACh} channels for a better understanding of the vagal HR control in such disease states.

We made two hypotheses regarding sympathetic effects on vagal HR control via the K_{ACh} channels. With respect to the speed of HR regulation, the indirect action of ACh relies on slower changes in intracellular cyclic AMP levels [10, 11]. In contrast, the direct action of ACh utilizes the faster membrane-delimited mechanisms of K_{ACh} channels and is believed to be independent of sympathetic control [12]. Accordingly, we first hypothesized that background sympathetic tone would not affect the *rapidity* of HR control provided by the K_{ACh} channel pathway. With respect to the magnitude of HR regulation, complex sympathovagal interactions can occur in autonomic HR control. Levy [13] termed the phenomenon that background sympathetic tone augmented vagal HR control "an accentuated antagonism." Kawada *et al.* [14] demonstrated that sympathovagal interaction bidirectionally increased the dynamic gain of HR control, even

Received on Jul 31, 2008; accepted on Sep 5, 2008; released online on Oct 10, 2008; doi:10.2170/physiolsci.RP011508
Correspondence should be addressed to: Masaki Mizuno, Department of Cardiovascular Dynamics, Advanced Medical Engineering Center, National Cardiovascular Center Research Institute, 5-7-1 Fujishirodai, Suita, Osaka, 565-8565 Japan. Tel: +81-6-6833-5012 (Ext. 2427), Fax: +81-6-6835-5403, E-mail: m-mizuno@ri.ncvc.go.jp

though the sympathetic and vagal systems affected mean HR antagonistically. Therefore we then hypothesized that background sympathetic tone would augment the *magnitude* of the HR response to vagal stimulation via K_{ACh} channels.

To test the above-mentioned hypotheses, we examined the dynamic and static transfer characteristics of the HR response to vagal stimulation using a selective K_{ACh} channel blocker tertiapin and concomitant cardiac sympathetic stimulation (CSS). Observation of significant interaction between tertiapin and CSS effects might allow us to deduce that background sympathetic tone influences the direct action of ACh via K_{ACh} channels.

MATERIALS AND METHODS

Surgical preparations. Animal care was consistent with "Guiding Principles for the Care and Use of Animals in the Field of Physiological Sciences" of the Physiological Society of Japan. All protocols were reviewed and approved by the Animal Subjects Committee of the National Cardiovascular Center. Seven Japanese white rabbits (2.7–3.2 kg body wt) were anesthetized using a mixture of urethane (250 mg/ml) and α-chloralose (40 mg/ml): an initial bolus dose of 2 ml/kg and a maintenance dose of 0.5 $ml \cdot kg^{-1} \cdot h^{-1}$. The rabbits were intubated and mechanically ventilated with oxygen-enriched room air. Arterial pressure (AP) was measured by a micromanometer (SPC-330A, Millar Instruments, Houston, TX, USA) inserted into the right femoral artery and advanced to the thoracic aorta. HR was measured with a cardiotachometer (model N4778, San-ei, Tokyo, Japan). A double-lumen catheter was introduced into the right femoral vein for continuous anesthetic and drug administration. Sinoaortic denervation was performed bilaterally to minimize changes in sympathetic efferent nerve activity via arterial baroreflexes. The main branches of the cardiac postganglionic sympathetic nerves were sectioned bilaterally through a midline thoracotomy. A pair of bipolar platinum electrodes was attached to the cardiac end of the sectioned right inferior cardiac sympathetic postganglionic nerve for tonic cardiac sympathetic nerve stimulation [15]. The vagi were sectioned bilaterally at the neck. Another pair of bipolar electrodes was attached to the cardiac end of the sectioned right vagus for vagal stimulation. Immersion of the stimulation electrodes and nerves in a mixture of white petroleum jelly (Vaseline) and liquid paraffin prevented the nerves from drying and also provided insulation. Body temperature was maintained at 38°C with a heating pad throughout the experiment.

Experimental protocols. The pulse duration of nerve stimulation was set at 2 ms. The stimulation amplitude of the right vagus was first adjusted in each animal to yield an HR decrease of ~50 beats/min at 10 Hz constant stimulation (1.6–6.0 V, 3.2 ± 1.7 V, mean ± SD) and fixed. The stimulation amplitude of the right cardiac sympathetic nerve was also adjusted in each animal to yield an HR increase of ~50 beats/min at 5 Hz constant stimulation (1.5–3.5 V, 2.2 ± 0.8 V) and fixed. Approximately 1 h elapsed after the completion of surgical preparation until stable hemodynamics were attained.

Dynamic protocol (n = 7). For an estimation of the dynamic transfer characteristics from vagal stimulation to the HR response, the right vagus was stimulated by a frequency-modulated pulse train for 10 min. The stimulation frequency was switched every 500 ms at either 0 or 10 Hz according to a binary white-noise signal. The power spectrum of the stimulation signal was reasonably constant up to 1 Hz. The transfer function was estimated up to 1 Hz because the reliability of estimation decreased as a result of the diminution of input power above this frequency. The selected frequency range spanned the frequency range of physiological interest sufficiently with respect to the dynamic vagal control of HR in rabbits.

Static protocol (n = 5). For an estimation of the static transfer characteristics between vagal stimulation and HR response, stepwise vagal stimulation was performed. Vagal stimulation frequency was increased to 20 Hz, from 5, in 5 Hz increments. Each frequency step was maintained for 60 s.

Pharmacological intervention. We used a selective K_{ACh} channel blocker tertiapin (Peptide Institute, Inc., Osaka, Japan) to block the direct action of ACh in vagal HR control. The dynamic and static characteristics of the heart rate response to vagal stimulation were estimated with and without CSS. After the tertiapin-free data were obtained, a bolus dose (30 nmol/kg iv) of tertiapin was administered. Fifteen min thereafter, the dynamic and static characteristics were estimated again, with and without CSS. The tertiapin-free data were obtained first in all animals because the long-lasting (>2 h) effects of tertiapin did not permit the acquisition of tertiapin-free data after the tertiapin administration. The order of dynamic and static protocols and the order of CSS application were randomly assigned in different animals. An intervening interval of more than 5 min was allowed between the dynamic and static protocols so that AP and HR returned their prestimulation values.

Data analysis. A 12-bit analog-to-digital converter was used to digitize the AP and HR recordings at 200 Hz, and the data were stored on the hard disk of a dedicated laboratory computer system. The dynamic transfer function from binary white-noise vagal stimulation to the HR response was estimated as follows. Input-output data pairs of the vagal stimulation frequency and HR were resampled at 10 Hz; then data pairs were partitioned into eight 50%-overlapping segments, each consisting of 1,024 data points. For each segment, the linear trend was subtracted and a Hanning window applied. A fast Fourier transform was then performed to obtain the frequency

spectra for vagal stimulation [$N(f)$] and HR [$HR(f)$] [16]. Over the eight segments, the power of the vagal stimulation [$S_{N\cdot N}(f)$], the power of the HR [$S_{HR\cdot HR}(f)$], and the cross-power between these two signals [$S_{N\cdot HR}(f)$] were ensemble averaged. Lastly, the transfer function [$H(f)$] from vagal stimulation to the HR response was estimated as follows [17, 18].

$$[H(f)] = \frac{S_{N\cdot HR}(f)}{S_{N\cdot N}(f)} \quad (1)$$

In previous studies [6, 14] the transfer function from vagal stimulation to HR response approximated a first-order, low-pass filter with a lag time; therefore the estimated transfer function was parameterized using the following mathematical model.

$$H(f) = \frac{-K}{1+\frac{f}{fc}j} e^{-2\pi f j L} \quad (2)$$

where K represents the dynamic gain (or, to be more accurate, the steady-state gain, in beats·min^{-1}·Hz^{-1}), fc denotes the corner frequency (in Hz), L denotes the lag time (in s), and f and j represent frequency and imaginary unit, respectively. The negative sign in the numerator indicates the negative HR response to vagal stimulation. The steady-state gain indicates the asymptotic value of the relative amplitude of HR response to vagal nerve stimulation when the frequency of input modulation approaches zero. The corner frequency represents the frequency of input modulation at which gain decreases by 3 dB from the steady-state gain in the frequency domain. The corner frequency reflects the rapidity of the HR response to vagal stimulation; the higher the corner frequency, the faster the HR response. The dynamic gain, corner frequency, and lag time were estimated by means of an iterative nonlinear least-squares regression. The phase shift of the transfer function indicates, with respect to the input signal, a lag or lead in the output signal normalized by its corresponding frequency of input modulation.

To quantify the linear dependence of the HR response on vagal stimulation, the magnitude-squared coherence function [$\mathrm{Coh}(f)$] was estimated as follows [17, 18].

$$[\mathrm{Coh}(f)] = \frac{|S_{N\cdot HR}(f)|^2}{S_{N\cdot N}(f)\cdot S_{HR\cdot HR}(f)} \quad (3)$$

Coherence values range from zero to unity. Unity coherence indicates perfect linear dependence between the input signals and output signals; in contrast, zero coherence indicates total independence between the two.

To facilitate the intuitive understanding of the system dynamic characteristics, we calculated the system step response of HR to 1 Hz nerve stimulation as follows. The system impulse response was derived from the inverse Fourier transform of $H(f)$. The system step response was then obtained from the time integral of the impulse response. The length of the step response was 51.2 s. We calculated the maximum step response by averaging the last 10 s of the step response. The time constant of the step response was calculated from the corner frequency of the corresponding transfer function using the following relationship.

$$\text{Time constant} = \frac{1}{2\cdot\Pi\cdot fc} \quad (4)$$

In this definition, the time constant is related inversely to the corner frequency without being influenced by the lag time.

The static transfer function from stepwise vagal stimulation to HR was estimated by averaging the HR data during the final 10 s of the 60 s stimulation at each stimulation step.

Statistical analysis. Values are mean ± SD. A two-way ANOVA, with drug and CSS as the main effects, was used to test the differences among parameters. $P < 0.05$ was considered significant.

RESULTS

Figure 1A shows recordings typical of the dynamic protocol. The top panels show HR under conditions of control (thin lines) and K_{ACh} channel blockade (thick lines), without (left) and with (right) CSS. The bottom panels show the binary white-noise signal used for vagal stimulation. Random vagal stimulation decreased HR intermittently. Tertiapin attenuated the HR variation in response to the dynamic vagal stimulation. CSS increased the mean level of HR and augmented HR variation in response to the dynamic vagal stimulation.

Figure 1B shows recordings typical of the static protocol. The top panels illustrate HR under conditions of control (thin lines) and K_{ACh} channel blockade (thick lines), without (left) and with (right) CSS. The bottom panels depict the vagal stimulation frequency. The stepwise vagal stimulation decreased HR in a stepwise manner. Tertiapin attenuated the bradycardic response to vagal stimulation regardless of CSS, which increased baseline HR and contributed to augment the response.

Dynamic protocol

The mean values of AP and HR before and during dynamic vagal stimulation are summarized in Table 1. This stimulation did not affect AP under any of the conditions, but it significantly decreased the mean HR except under the conditions of K_{ACh} channel blockade without CSS, which increased the mean HR ($P < 0.01$), but not the mean AP, both before and during vagal stimulation.

Figure 2A illustrates the dynamic transfer functions characterizing the vagal HR control averaged for all animals under conditions of control (thin lines) and K_{ACh} channel blockade (thick lines), without (left) and with (right) CSS. Gain plots, phase plots, and coherence functions are shown. Note that the frequency axes of these plots indicate the modulation frequency of the random

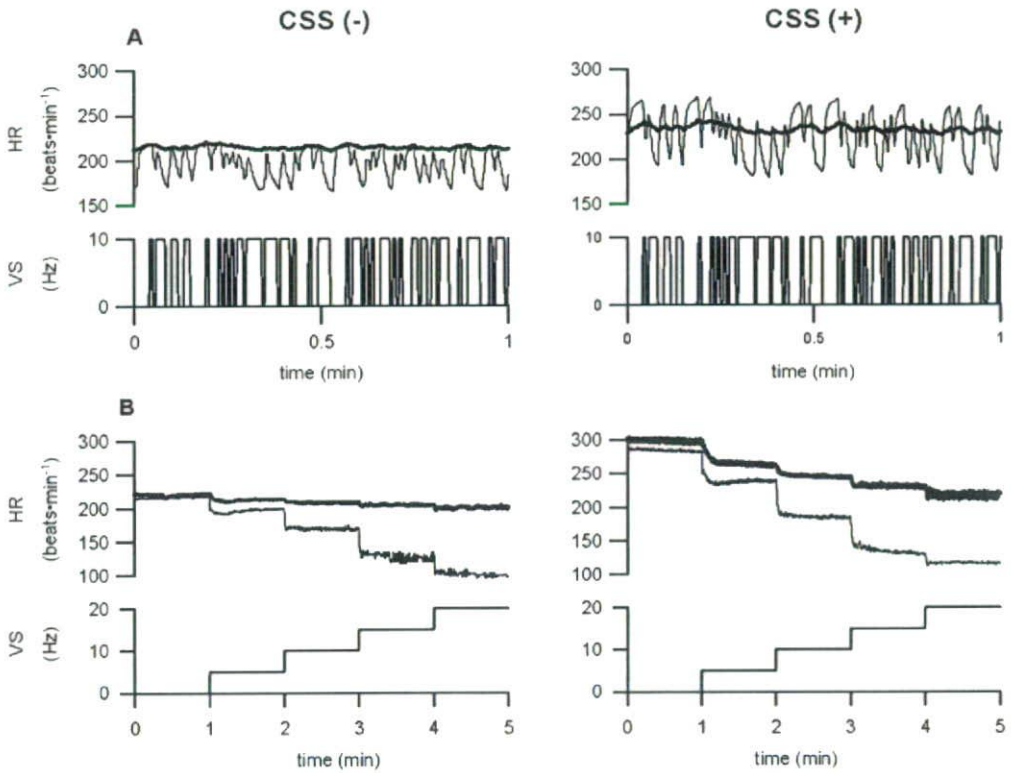

Fig. 1. A: Representative recordings of HR obtained utilizing binary white-noise vagal stimulation (top) and the corresponding vagal stimulation (VS; bottom) without (left) and with (right) CSS. Thin line, control; thick line, K_{ACh} channel blockade with tertiapin (30 nmol·kg^{-1} iv). **B**: Representative recordings of HR obtained utilizing stepwise vagal stimulation (top) and the corresponding VS (bottom) without (left) and with (right) CSS, which increased the basal HR and the amplitude of HR variation in both binary white-noise and stepwise vagal stimulations. A K_{ACh} channel blockade attenuated the amplitude of HR variation and the speed of the response of HR to vagal stimulation regardless of CSS.

Table 1. Effects of tertiapin infusion and CSS on AP and HR before and during dynamic vagal stimulation.

	CSS (–)		CSS (+)		Comparison factors		
	Control	Tertiapin	Control	Tertiapin	Drug	CSS	Interaction
AP, mmHg							
Before stimulation	82.2 ± 16.8	76.7 ± 20.1	90.5 ± 13.8	81.8 ± 16.6	0.022	0.641	0.546
During stimulation	80.2 ± 18.4	76.6 ± 21.4	81.8 ± 14.8	75.9 ± 19.0	0.144	0.962	0.709
HR, beats·min^{-1}							
Before stimulation	247.8 ± 20.1	247.9 ± 30.8	312.2 ± 15.6	307.4 ± 20.9	0.521	<0.001	0.494
During stimulation	211.9 ± 17.5**	228.3 ± 23.4	244.3 ± 33.3**	248.1 ± 30.7**	0.026	<0.001	0.308

Values are means ± SD (n = 7). CSS, cardiac sympathetic stimulation; AP, arterial pressure; HR, heart rate. **P < 0.01 vs. corresponding values before stimulation. Tertiapin was infused at 30 nmol/kg iv.

input signal and not the vagal stimulation frequency itself. Table 2 summarizes parameters of the transfer function at 0.01, 0.1, 0.5, and 1 Hz and also those of the step response. Tertiapin attenuated the dynamic gain compared with the control conditions regardless of CSS. The phase approached $-\Pi$ radians at the lowest frequency and lagged with increasing frequency under the control conditions. Tertiapin increased the phase delay in the frequency range from 0.01 to 1 Hz. Coherence was near unity in the overall frequency range under the control conditions. A decrease in the coherence function from unity was noted >0.6 Hz under the condition of the K_{ACh} channel blockade, which was reversed by CSS.

Figure 2B shows the calculated step response of HR to vagal stimulation averaged for all animals under the conditions of control (thin lines) and K_{ACh} channel blockade

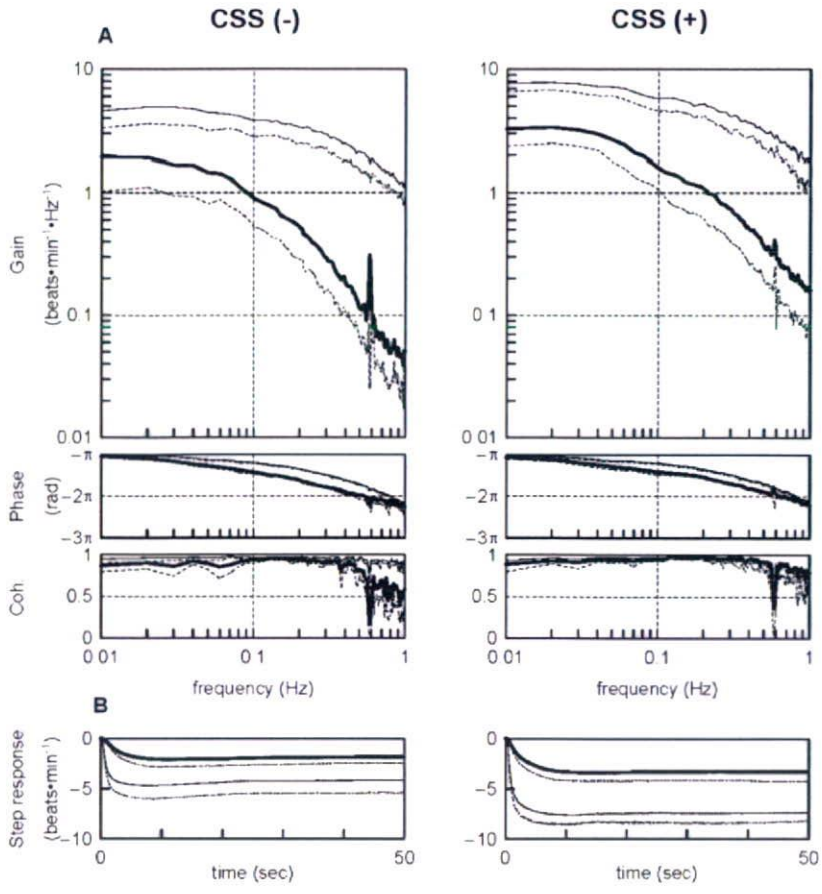

Fig. 2. A: Dynamic transfer function relating vagal stimulation to the HR responses averaged from all animals (pooled data; n = 7) without (left) and with (right) CSS. Solid lines, means; dashed lines, −SD. Thin line, control; thick line, a K_{ACh} channel blockade with tertiapin (30 nmol·kg^{-1} iv). Top: gains; middle: phase shifts; bottom: coherence (Coh) functions. Tertiapin decreased transfer gain and increased the phase shift with increasing frequency. Cardiac sympathetic stimulation increased transfer gain both under control conditions and under conditions of a K_{ACh} channel blockade without affecting the phase shift. **B**: Calculated step response to 1 Hz tonic vagal stimulation averaged from all animals (pooled data; n = 7) without (left) and with (right) CSS. Solid lines, means; dashed lines, −SD. Thin line, control; thick line, K_{ACh} channel blockade with tertiapin (30 nmol·kg^{-1} iv). The K_{ACh} channel blockade decreased the maximum step response and slowed the initial step response. CSS increased the maximum step response both under control conditions and under conditions of a K_{ACh} channel blockade without affecting the initial response (see Table 2).

Table 2. Effects of tertiapin infusion and CSS on parameters of the transfer function and step response.

	CSS (−)		CSS (+)		Comparison factors		
	Control	Tertiapin	Control	Tertiapin	Drug	CSS	Interaction
Gain, beats·min^{-1}·Hz^{-1}							
0.01 Hz	4.58 ± 1.26	2.21 ± 0.97	7.73 ± 1.15	3.28 ± 0.92	<0.001	0.001	0.007
0.1 Hz	3.81 ± 1.01	1.10 ± 0.43	5.82 ± 1.28	1.60 ± 0.54	<0.001	0.007	0.015
0.5 Hz	2.12 ± 0.64	0.16 ± 0.07	3.08 ± 0.82	0.36 ± 0.17	<0.001	0.013	0.081
1 Hz	1.09 ± 0.27	0.08 ± 0.03	1.73 ± 0.61	0.16 ± 0.08	<0.001	0.019	0.044
Phase, rad							
0.01 Hz	3.10 ± 0.04	2.99 ± 0.11	2.99 ± 0.11	2.92 ± 0.14	0.037	0.077	0.579
0.1 Hz	2.52 ± 0.08	1.78 ± 0.17	2.52 ± 0.11	1.83 ± 0.25	<0.001	0.757	0.719
0.5 Hz	0.91 ± 0.13	0.03 ± 0.27	0.90 ± 0.10	0.35 ± 0.10	<0.001	0.011	0.056
1 Hz	−0.56 ± 0.33	−0.81 ± 0.21	−0.41 ± 0.26	−0.64 ± 0.18	0.014	0.159	0.905
Coherence							
0.01 Hz	0.95 ± 0.05	0.87 ± 0.07	0.93 ± 0.04	0.89 ± 0.09	0.005	0.947	0.424
0.1 Hz	0.96 ± 0.03	0.94 ± 0.04	0.97 ± 0.01	0.95 ± 0.02	0.004	0.440	0.835
0.5 Hz	0.96 ± 0.02	0.83 ± 0.08	0.91 ± 0.08	0.93 ± 0.04	0.026	0.259	0.006
1 Hz	0.90 ± 0.07	0.59 ± 0.16	0.78 ± 0.15	0.79 ± 0.12	0.017	0.312	0.011
Maximum step response, beats·min^{-1}	−4.2 ± 1.2	−1.8 ± 0.6	−7.4 ± 0.9	−3.3 ± 0.9	<0.001	<0.001	0.005
Time constant, s	0.63 ± 0.09	3.34 ± 0.55	0.74 ± 0.18	3.18 ± 1.10	<0.001	0.913	0.560

Values are means ± SD (n = 7). CSS, cardiac sympathetic stimulation. Tertiapin was infused at 30 nmol/kg iv.

Table 3. Effects of tertiapin infusion and CSS on parameters of the transfer function relating dynamic vagal stimulation to HR.

	CSS (–)		CSS (+)		Comparison factors		
	Control	Tertiapin	Control	Tertiapin	Drug	CSS	Interaction
Dynamic gain, beats·min^{-1}·Hz^{-1}	4.6 ± 1.1	2.3 ± 0.9	7.3 ± 1.1	3.6 ± 1.0	<0.001	<0.001	0.037
Corner frequency, Hz	0.26 ± 0.04	0.05 ± 0.01	0.23 ± 0.06	0.06 ± 0.02	<0.001	0.439	0.1613
Lag time, s	0.38 ± 0.04	0.45 ± 0.04	0.34 ± 0.04	0.38 ± 0.03	<0.001	0.002	0.2776

Values are means ± SD (n = 7). CSS, cardiac sympathetic stimulation; HR, heart rate. Tertiapin was infused at 30 nmol/kg iv.

(thick lines), without (left) and with (right) CSS. Tertiapin slowed the transient response and attenuated the HR response to vagal stimulation in the time domain. CSS did not affect the time constant, though it augmented the maximum step response. A significant interaction was observed between the tertiapin and CSS effects in the maximum step response, but not in the time constant (Table 2).

The fitted parameters of the transfer functions are summarized in Table 3. Tertiapin significantly decreased the dynamic gain and the corner frequency and significantly increased the lag time. Conversely, CSS significantly increased the dynamic gain and significantly decreased the lag time. A significant interaction was observed between the tertiapin and CSS effects only in dynamic gain.

Static protocol

Figure 3A summarizes changes in HR in response to stepwise vagal stimulation without (left) and with (right) CSS, which increased basal HR obtained at 0 Hz vagal stimulation by approximately 50 beats·min^{-1}. Tertiapin significantly attenuated the bradycardic response to vagal stimulation regardless of CSS. The magnitude of attenuation (i.e., the difference between the open and closed symbols) became greater as the vagal stimulation frequency increased.

Figure 3B demonstrates the HR reduction obtained under four conditions at each frequency. To aid an intuitive understanding, the tertiapin condition is designated as D(–) in this panel because tertiapin blocked the direct action of ACh. S(+) indicates the presence of CSS. At 5 Hz vagal stimulation frequency, the direct action alone S(–)D(+) significantly augmented the HR reduction, as depicted by the diagonal hatch. CSS alone S(+)D(–) also significantly augmented the HR reduction, as depicted by the vertical hatch. The augmentation of the HR reduction obtained by S(+)D(+) exceeded the simple summation of the diagonal hatch and vertical hatch, suggesting that the effect of the direct action was enhanced by CSS (depicted in the solid rectangle). The positive interaction waned at 10 Hz vagal stimulation and disappeared at 15 and 20 Hz vagal stimulation. That is, the simple summation of the diagonal hatch and vertical hatch largely explained the augmentation of the HR reduction attained by S(+)D(+) at 15 and 20 Hz vagal stimulation.

DISCUSSION

We have examined the effect of background sympathetic tone on the direct action of ACh through K_{ACh} channels by examining the dynamic and static transfer characteristics. The major findings in the present study are that the bradycardic response to vagal stimulation via the K_{ACh} channels was augmented by concomitant CSS, depending on vagal stimulation frequency. The rapidity of vagal HR control obtained by the K_{ACh} channels, however, was not affected by CSS. These findings support our hypotheses and demonstrated, for the first time to our knowledge, the existence of an accentuated antagonism in the direct action of ACh through the K_{ACh} channels.

Effect of CSS on the rapidity of vagal HR control via K_{ACh} channels

Our results indicate that the rapidity of the vagal HR control via the K_{ACh} channels was not affected by background sympathetic tone. In the transfer function, the phase values were significantly more delayed by the K_{ACh} channel blockade in the frequency range from 0.01 to 1 Hz in agreement with our previous study [6]. In contrast, CSS did not affect the phase characteristics, in which no significant interaction was observed at each frequency (Table 2). Moreover, the calculated step response clearly demonstrated that tertiapin significantly prolonged the time constant by >2 s, whereas CSS did not affect it (Fig. 2B and Table 2).

Changes in fitted parameters of the transfer function from vagal stimulation to HR also support our first hypothesis that CSS does not affect the rapidity of the vagal HR control mediated by the K_{ACh} channels. Tertiapin decreased the corner frequency to a similar degree without or with CSS, which did not affect the corner frequency. On the other hand, tertiapin prolonged the lag time, whereas CSS shortened it (Table 3). However, changes in the lag time caused by tertiapin or CSS were less than 0.1 s and might

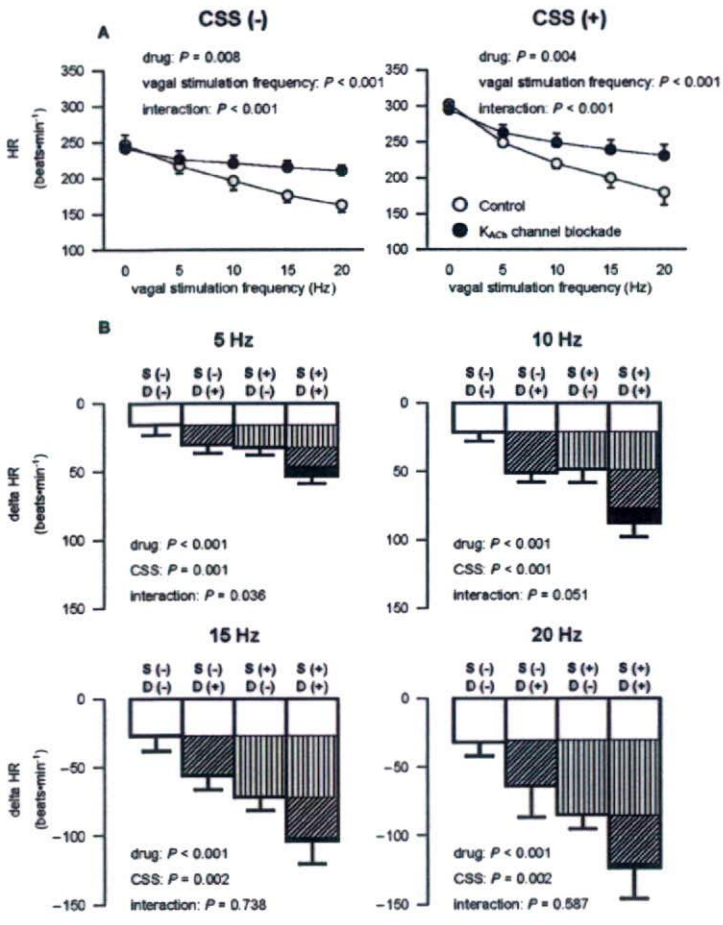

Fig. 3. A: Static HR responses relating stepwise vagal stimulation averaged from all animals (pooled data; n = 5) without (left) and with (right) CSS. A K_{ACh} channel blockade decreases the static HR response, and the static reductions in the bradycardic effect were greater at higher stimulation frequencies in both conditions. **B**: Changes in HR responses from baseline to vagal stimulation at 5 Hz (top left), 10 Hz (top right), 15 Hz (bottom left), and 20 Hz (bottom right) averaged from all animals (pooled data; n = 5). To aid an intuitive understanding, the tertiapin condition was designated as D(–) in this panel because tertiapin blocked the direct action of ACh. S(+) indicates the presence of CSS. Significant interaction and a tendency towards significant interaction (P = 0.051) were obtained at 5 and 10 Hz vagal stimulation, respectively, but not at 15 and 20 Hz vagal stimulation.

be insignificant in terms of physiological HR control.

Effect of CSS on the gain of vagal HR control via K_{ACh} channels

Because the direct action of ACh via K_{ACh} is considered to be independent of sympathetic control [12], an accentuated antagonism is unlikely to occur in the direct action. However, because the interbeat interval is determined by the pacemaker potential of the sinus node cells, which in turn depends on all of the potassium, sodium, and calcium currents, there could be interaction between the K_{ACh} channel pathway and background sympathetic tone when we observe the HR response. Changes in the sodium current and/or calcium current induced by background sympathetic tone would modify the effect of changes in the potassium current through the K_{ACh} channels.

Our results indicate that accentuated antagonism occurred, affecting the direct action of ACh in the range of mild vagal stimulation as follows. In the dynamic protocol that was carried out with a mean vagal stimulation frequency of 5 Hz, significant positive interaction was observed between the tertiapin and CSS effects, affecting the dynamic gain as well as the calculated maximum step response (Table 2), suggesting that the effect of the K_{ACh} channel pathway was enhanced during CSS. The static protocol also showed significant positive interaction at 5 Hz vagal stimulation (Fig. 3B). The augmentation of the bradycardic response to vagal stimulation gained by the direct action of ACh through the K_{ACh} channels was enhanced under concomitant CSS.

The reason for the absence of a positive interaction between the tertiapin and CSS effects at 15 and 20 Hz vagal stimulation is unclear (Fig. 3B). One possible explanation is the curvilinearity of the HR response to vagal stimulation. In the right panel of Fig. 3A, the tertiapin-free control data (open symbols), which correspond to S(+)D(+) in Fig. 3B, showed the steepest slope at the 0–5 Hz vagal stimulation step. The slope became shallower as the vagal stimulation frequency increased, suggesting a saturation phenomenon of HR reduction in response to vagal stimulation. It is very likely that such curvilinearity masked possible positive interaction between CSS and the direct action of ACh in determining the HR reduction during 15 and 20 Hz vagal stimulation. Accentuated antagonism in the direct action of ACh through K_{ACh} channels might therefore operate under balanced conditions of sympa-

thetic and vagal nerve activities.

The existence of an accentuated antagonism in the direct action of ACh through the K_{ACh} channels could be explained by macromolecular signaling complexes in which G protein-gated inwardly rectifying potassium (GIRK) channels are physically associated with signaling partner regulated by different G protein-coupled receptors (GPCRs) [19, 20]. Cardiac sympathetic stimulation simultaneously activates several different GPCRs: α-adrenergic, β1-adrenergic, and β2-adrenergic receptors. Notably, the β1-adrenergic receptor is coupled to downstream kinase, protein kinase A (PKA). The β-adrenergic signaling via PKA phosphorylation increases the activity of K_{ACh} channels [21, 22]. Taken together, β-adrenergic receptors might augment the activity of K_{ACh} channels via a PKA-dependent mechanism.

Limitations

This study has several limitations. First, the data was obtained from anesthetized animals. Since anesthesia would affect the autonomic tone, the results may not be directly applicable to conscious animals. However, because we cut and stimulated the right cardiac sympathetic and vagal nerves, changes in autonomic outflow associated with anesthesia might not have significantly affected the present results.

Second, we blocked the K_{ACh} channels to examine the effect of background sympathetic tone on the direct effect of ACh through the K_{ACh} channels. On the other hand, if we had blocked the indirect effect of ACh through the cyclic AMP pathway, leaving the direct effect of ACh intact, and then examined the effect of background sympathetic tone on the HR response to vagal stimulation, the results might have been excessively straightforward. However, we could find no blocker for the indirect effect of ACh alone that was suitable for in vivo study at present. Further studies are required to directly examine the effect of background sympathetic tone on the direct effect of ACh through the K_{ACh} channels.

In conclusion, concomitant CSS affected no parameters of rapidity (i.e., the corner frequency in the frequency domain and the time constant in the time domain) of vagal HR control via K_{ACh} channels. Moreover, HR reduction in response to vagal stimulation via K_{ACh} channels was augmented by concomitant sympathetic stimulation at 5 Hz vagal stimulation. These findings suggest that the rapidity of response of the vagal HR control via K_{ACh} channels is invariant with respect to background sympathetic tone, and that the magnitude of vagal HR control via K_{ACh} channels is affected by background sympathetic tone in vivo.

This study was supported by Health and Labour Sciences Research Grants H15-Physi-001, H18-Nano-Ippan-003, and H18-Iryo-Ippan-023 from the Ministry of Health, Grants-in-Aid for Scientific Research promoted by the Ministry of Education, Culture, Sports, Science and Technology in Japan 18591992, 19700559, and by the Ground-based Research Announcement for Space Utilization project promoted by the Japan Space Forum. This study was also supported by an Industrial Technology Research Grant Program in 06B44524a from the New Energy and Industrial Technology Development Organization of Japan.

REFERENCES

1. Luetje CW, Tietje KM, Christian JL, Nathanson NM. Differential tissue expression and developmental regulation of guanine nucleotide binding regulatory proteins and their messenger RNAs in rat heart. J Biol Chem. 1988;263:13357-65.
2. Sunahara RK, Dessauer CW, Gilman AG. Complexity and diversity of mammalian adenylyl cyclases. Annu Rev Pharmacol Toxicol. 1996;36:461-80.
3. Huang CL, Slesinger PA, Casey PJ, Jan YN, Jan LY. Evidence that direct binding of G beta gamma to the GIRK1 G protein-gated inwardly rectifying K+ channel is important for channel activation. Neuron. 1995;15:1133-43.
4. Sakmann B, Noma A, Trautwein W. Acetylcholine activation of single muscarinic K+ channels in isolated pacemaker cells of the mammalian heart. Nature. 1983;303:250-3.
5. Yamada M, Inanobe A, Kurachi Y. G protein regulation of potassium ion channels. Pharmacol Rev. 1998;50:723-60.
6. Mizuno M, Kamiya A, Kawada T, Miyamoto T, Shimizu S, Sugimachi M. Muscarinic potassium channels augment dynamic and static heart rate responses to vagal stimulation. Am J Physiol Heart Circ Physiol. 2007;293:H1564-70.
7. Negrão CE, Rondon MU, Tinucci T, Alves MJ, Roveda F, Braga AM, Reis SF, Nastari L, Barretto AC, Krieger EM, Middlekauff HR. Abnormal neurovascular control during exercise is linked to heart failure severity. Am J Physiol Heart Circ Physiol. 2001;280:H1286-92.
8. Mancia G, Grassi G, Giannattasio C, Seravalle G. Sympathetic activation in the pathogenesis of hypertension and progression of organ damage. Hypertension. 1999;34:724-8.
9. Seals DR, Bell C. Chronic sympathetic activation: consequence and cause of age-associated obesity? Diabetes. 2004;53:276-84.
10. Hartzell HC, Méry PF, Fischmeister R, Szabo G. Sympathetic regulation of cardiac calcium current is due exclusively to cAMP-dependent phosphorylation. Nature. 1991;351:573-6.
11. Irisawa H, Brown HF, Giles W. Cardiac pacemaking in the sinoatrial node. Physiol Rev. 1993;73:197-227.
12. Breitwieser GE, Szabo G. Uncoupling of cardiac muscarinic and beta-adrenergic receptors from ion channels by a guanine nucleotide analogue. Nature. 1985;317:538-40.
13. Levy MN. Sympathetic-parasympathetic interactions in the heart. Circ Res. 1971;29:437-45.
14. Kawada T, Ikeda Y, Sugimachi M, Shishido T, Kawaguchi O, Yamazaki T, Alexander J Jr, Sunagawa K. Bidirectional augmentation of heart rate regulation by autonomic nervous system in rabbits. Am J Physiol. 1996;271:H288-95.
15. Kawada T, Uemura K, Kashihara K, Jin Y, Li M, Zheng C, Sugimachi M, Sunagawa K. Uniformity in dynamic baroreflex regulation of left and right cardiac sympathetic nerve activities. Am J Physiol Regul Integr Comp Physiol. 2003;284:R1506-12.
16. Brigham E. FFT transform applications. In: The Fast Fourier Transform and its applications. Englewood Cliffs, NJ: Prentice Hall; 1988. p. 167-203.
17. Bendat J, Piersol A. Single-input/output relationships. In: Random data: analysis and measurement procedures (3rd edition). New York: Wiley; 2000. p. 189-217.
18. Marmarelis P, Marmarelis V. The white noise method in system identification. In: Analysis of physiological systems. New York: Plenum; 1978. p. 131-221.
19. Lavine N, Ethier N, Oak JN, Pei L, Liu F, Trieu P, Rebois RV, Bouvier M, Hebert TE, Van Tol HH. G protein-coupled receptors form stable complexes with inwardly rectifying potassium channels and adenylyl cyclase. J Biol Chem. 2002;277:46010-9.
20. Nikolov EN, Ivanova-Nikolova TT. Coordination of membrane excitability through a GIRK1 signaling complex in the atria. J Biol Chem. 2004;279:23630-6.
21. Kim D. Beta-adrenergic regulation of the muscarinic-gated K+ channel via cyclic AMP-dependent protein kinase in atrial cells. Circ Res. 1990;67:1292-8.
22. Müllner C, Vorobiov D, Bera AK, Uezono Y, Yakubovich D, Frohnwieser-Steinecker B, Dascal N, Schreibmayer W. Heterologous facilitation of G protein-activated K(+) channels by beta-adrenergic stimulation via cAMP-dependent protein kinase. J Gen Physiol. 2000;115:547-58.

30th Annual International IEEE EMBS Conference
Vancouver, British Columbia, Canada, August 20-24, 2008

Modification of Autonomic Balance by Electrical Acupuncture does not Affect Baroreflex Dynamic Characteristics

Masaru Sugimachi, *Member, IEEE*, Toru Kawada,
Hiromi Yamamoto, Atsunori Kamiya,
Tadayoshi Miyamoto, and Kenji Sunagawa, *Member, IEEE*

Abstract— *Background:* **We have demonstrated that modification of autonomic balance by electrical vagal stimulation delays progression of cardiac dysfunction and cardiac remodeling, and prolongs survival in rats with severe heart failure. We have also shown that we were able to modify autonomic balance by electrical acupuncture at the acupoint of Zusanli, potentially applicable for the treatment of heart failure. We examined the effect of the acupuncture on the dynamic characteristics of the baroreflex system to exclude the possible deleterious effect on orthostatic tolerance.**

Method: **In anesthetized 8 and 6 rabbits, we examined static and dynamic characteristics of baroreflex, respectively, with and without electrical acupuncture (1 Hz, 5 mA, and 5msec). Dynamic characteristics were examined by imposing pseudorandom binary changes in isolated carotid sinus pressure.**

Results: **With the stimulation condition to decrease arterial blood pressure and sympathetic nerve activity (resulted form decreased response range of neural arc), either of the dynamic characteristics of neural arc or those of peripheral arc did not change by electrical acupuncture at Zusanli.**

Conclusion: **We conclude that application of electrical acupuncture at Zusanli can suppress sympathetic nerve activity but does not affect the dynamic characteristics of the arterial baroreflex system, indicating no deleterious effect on orthostatic tolerance.**

Manuscript received April 7, 2008. This work was supported in part by Health and Labour Sciences Research Grants (H19-nano-ippan-009, H15-physi-001) from the Ministry of Health Labour and Welfare of Japan, and by the Program for Promotion of Fundamental Studies in Health Science of the National Institute of Biomedical Innovation.

M. Sugimachi, D. Michikami, T. Kawada, H. Yamamoto, and A. Kamiya are with the National Cardiovascular Center Research Institute, Suita, Osaka 5658565, Japan (corresponding author Masaru Sugimachi to provide phone: +81-6-6833-512; fax: +81-6-6835-5403; e-mail: su91mach@ri.ncvc.go.jp).

D. Michikami is supported by a postdoctoral program by Japan Association for the Advancement of Medical Equipment.

T. Miyamoto is with Morinomiya University of Medical Sciences, Osaka 5590034 Japan. (e-mail: miyamoto@morinomiya-u.ac.jp).

K. Sunagawa is with Kyushu University Graduate School of Medical Sciences, Fukuoka 8128582 Japan. (e-mail: sunagawa@cardiol.med.kyushu-u.ac.jp).

I. INTRODUCTION

IT is widely accepted that chronic heart failure involves not only abnormal structural and functional changes of heart and vessels themselves, but also abnormal changes in cardiovascular regulation. The fact that all successful cardiovascular drugs (ACE inhibitors, beta-adrenergic blockers, angiotensin receptor blockers, and aldosterone inhibitors) recently developed to treat heart failure are aimed at antagonizing neurohumoral activation has supported this.

We have shown that modification of autonomic balance by direct electrical vagal stimulation has inhibited cardiac remodeling, further deterioration of cardiac function, and improved survival in rat model of post-infarction severe chronic heart failure [1]. Because of the poor prognosis of chronic heart failure even with the use of combination of medical therapy, device-based therapy and the current state-of-art therapeutic modalities, such as cardiac transplantation, artificial heart, development of an additional therapeutic strategy attacking the abnormal cardiovascular regulation seems of great value to help still unsaved patients.

We have also shown in the last meeting that we were able to modify autonomic balance by electrical acupuncture at the acupoint of Zusanli, which is potentially applicable to treat heart failure. The less invasive nature of the acupuncture would greatly enhance its widespread use.

In this article, we have examined the effect of the acupuncture on the dynamic characteristics of the baroreflex system to ensure that there is no deleterious effect on orthostatic tolerance. The results indicated that electrical acupuncture is able to suppress sympathetic nerve activity but does not affect the dynamic characteristics of the arterial baroreflex system.

II. MODEL AND METHODS

A. Animal Experiments

We used 8 rabbits (Japanese White) to examine the effects of electrical acupuncture on open-loop static characteristics of baroreflex system. The effects of electrical acupuncture on open-loop dynamic characteristics were examined in other 6 rabbits.

978-1-4244-1815-2/08/$25.00 ©2008 IEEE.

In both protocols, rabbits were cared for in accordance with the Guiding Principles for the Care and Use of Animals in the Field of Physiological Sciences approved by the Physiological Society of Japan. These animals were anesthetized by a mixture of urethane (250 mg/ml) and α-chloralose (40 mg/ml) with an initial dose of 2 ml/kg (iv) and additional doses to maintain an appropriate level of anesthesia. Rabbits were mechanically ventilated with oxygen-enriched room air. Pancuronium bromide (0.1 mg/kg), a muscle relaxant was administered to prevent contaminating muscular activities.

A catheter-tipped micromanometer was inserted into a femoral artery to measure arterial blood pressure. After thoracotomy, we identified a left cardiac sympathetic nerve and the peripheral end was cut. Its efferent activity was recorded by a pair of stainless steel wire electrodes attached to the central end. We used silicone glue (Kwik-Sil, World Precision Instruments, Sarasota, FL) to fix the electrode, to provide insulation and to prevent the nerve from drying. We band-pass filtered the electrical signal at 150–1000 Hz and full-wave rectified, and low-pass filtered at a cutoff frequency of 30 Hz to quantify nerve activity.

To open the negative feedback loop, we isolated both carotid sinuses from the systemic circulation. We filled the isolated carotid sinuses with warmed physiological saline for longer preservation of baroreflex function. The blind-sac carotid sinuses were connected to a servo-controlled piston pump (model ET-126A, Labworks, Costa Mesa, CA) to control the pressure imposed on baroreceptors. Although being unphysiological and making baroreflex gain lower, it was necessary to cut bilateral vagal nerves and bilateral aortic depressor nerves to make baroreflex system fully open-loop condition.

Signals such as arterial blood pressure (AP), integrated sympathetic nerve activity (SNA), and carotid sinus pressure (CSP) were simultaneously digitized by a 12-bit analog-to-digital converter interfaced with a laboratory computer, and were stored on a hard disk for offline analysis. We used an arbitrary unit for nerve activity.

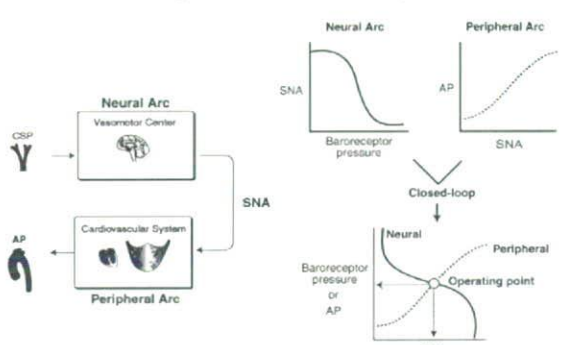

Fig. 1. Decoupling and recoupling of the arterial baroreflex system into neural arc and peripheral arc. CSP, carotid sinus pressure; AP, arterial blood pressure; SNA, sympathetic nerve activity.

B. Method to Identify Static Open-loop Characteristics of Baroreflex System

We have opened (see above) the total negative feedback loop of the arterial baroreflex system, and subdivided it into two subsystems. The two subsystems include the "neural arc" (which in turn includs baroreceptor and vasomotor center) and the "peripheral arc" (which in turn includes various sympathetic effectors). The neural arc corresponds to the controller and the peripheral arc corresponds to the plant of the baroreflex feedback system [2].

To quantify the static characteristics, we imposed stepwise change in CSP from 40 mmHg to 160mmHg with an increment of 20 mmHg. The particular CSP level was maintained for 60 seconds and the steady-state CSP, SNA, and AP were quantified by averaging the digitized values for the last 10 seconds.

We have characterized the neural arc by the relationship between CSP and SNA. We have characterized the peripheral arc by the relationship between SNA and AP. By recoupling these curves we can determine the operating point of the baroreflex system under the closed-loop condition by the intersection between the neural and peripheral arc curves.

C. Method to Identify Dynamic Open-loop Characteristics of Baroreflex System

We identified the dynamic characteristics of baroreflex, with or without electrical acupuncture. We imposed CSP changes around the respective closed-loop operating point with the amplitude of 20 mmHg according to a pseudorandom binary sequence.

The wideband nature of white noise input allows estimation of the wideband system dynamic properties. In addition, we ensemble-averaged the input power and cross power across multiple segments to reduce the statistical variance [3, 4].

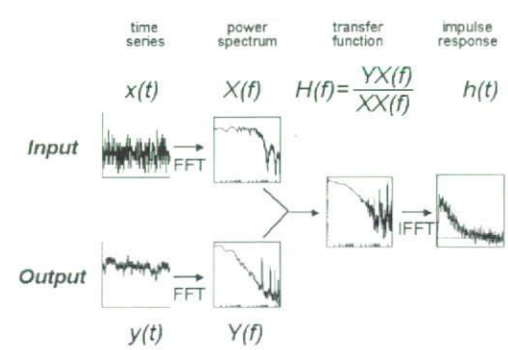

Fig. 2. Method to identify dynamic characteristics of a system. x(t), input signal; y(t), output signal; X(f) and Y(f), amplitude spectrum of x(t) and y(t), respectively; XX(f) and YX(f), ensemble-averaged input power spectrum and cross power (between input and output) spectrum, respectively; H(f), transfer function; h(t), impulse response.

We identified neural arc dynamic characteristics by analyzing CSP as input and SNA as output. We also identified peripheral arc dynamic characteristics by analyzing SNA as input and AP as output. Total baroreflex dynamic characteristics were obtained by analyzing CSP as input and AP as output.

In reference to Fig. 2, both input [x(t)] and output [y(t)] signals are divided into multiple segments. These data are subjected to frequency analysis using a fast Fourier transform (FFT) algorithm [X(f) and Y(f)]. The calculated input power and cross power (between input and output signals) are ensemble-averaged across segments to reduce variance [XX(f) and YX(f)]. Finally the transfer function [H(f)] is obtained by dividing the ensembled cross power by the ensembled input power. The impulse response [h(t)] is calculated by the inverse FFT of the transfer function.

D. Electrical Acupuncture

We have performed electrical acupuncture at Zusanli, i.e., the one-fifth point (from the knee) with the use of a pair of stainless steel wires (0.2 mm in diameter). The midpoint of the knee-ankle distance of approximately 30–35 mm served as the reference electrode. These needles were inserted to a depth of 10 mm in the skin and underlying muscle (the tibialis anterior muscle) [5].

The effects of Zusanli stimulation on baroreflex neural and peripheral arc characteristics were studied with the stimulation condition of 1 Hz, 5 mA, and 5msec. The stimulation condition is based on preliminary experiments.

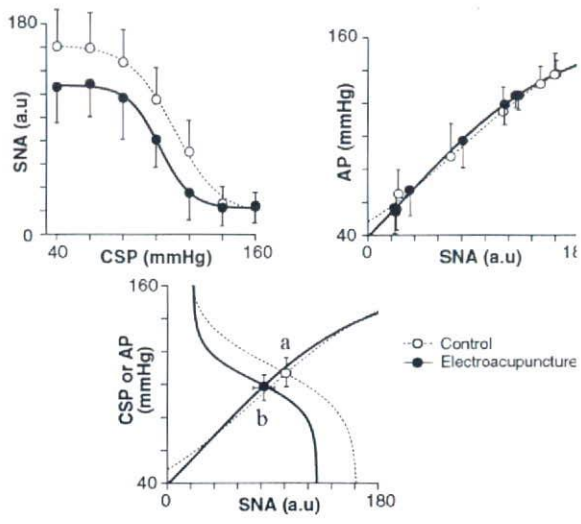

Fig. 3. Effect of electrical acupuncture on neural arc (top left) and peripheral arc (top right) static characteristics of arterial baroreflex, superimposed neural and peripheral arc curves (bottom). CSP, carotid sinus pressure; AP, arterial blood pressure; SNA, sympathetic nerve activity; solid line, with electrical acupuncture; dashed line, without electrical acupuncture, error bars, 1SD.

III. Results

A. Effects on Static Characteristic

The response range of SNA for the CSP change of 40-160 mmHg was obviously decreased with Zusanli stimulation (neural arc, Fig. 3 top left). The peripheral arc does not seem to change by Zusanli stimulation (Fig. 3 top right). These changes resulted in the decreased AP and SNA at the closed-loop operation point (Fig. 3 bottom).

B. Effects on Dynamic Characteristic

Fig. 4 exemplifies the time series of data obtained before and during pseudorandom changes in CSP. We imposed changes in CSP of ±20 mmHg around the respective closed-loop operating point.

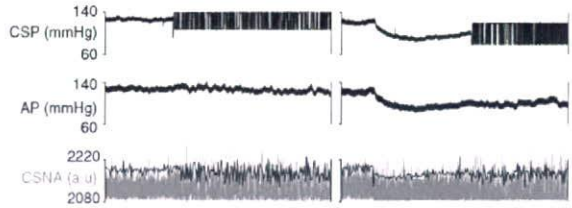

Fig. 4. An example of time series before and during changes in carotid sinus pressure according to pseudorandom binary sequence, with (right) and without (left) electrical acupuncture. CSP, carotid sinus pressure; AP, arterial blood pressure; CSNA, cardiac sympathetic nerve activity.

Changes in dynamic characteristics of neural arc, peripheral arc, and total loop by electrical acupuncture are shown in Fig. 5. As shown in the figure, transfer functions (dynamic characteristics) of neural arc, peripheral arc, and total loop were superimposable.

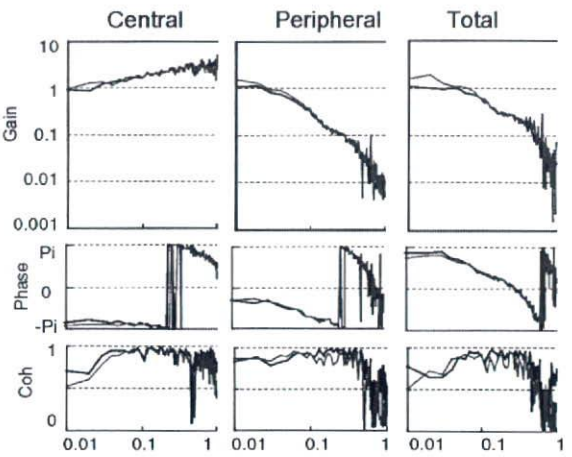

Fig. 5. Transfer functions (dynamic characteristics) of neural arc (left), peripheral arc (middle), and total loop (right) of baroreflex, with (gray) and without (black) electrical acupuncture. From top to bottom, gain, phase, and squared magnitude of coherence are shown.

IV. Discussion

We have repeatedly demonstrated that electrical vagal stimulation was successful in retarding further deterioration of cardiac function and progression of cardiac remodeling in rats with severe heart failure. This therapeutic method is also capable of prolonging survival in heart failure rats. These effects were believed to be mediated by the modification of autonomic balance.

Based on these results, several groups of investigators are developing an implantable vagal neurostimulators to apply this method for the human use; the invasive nature of the implantable device is likely to limit its widespread use, especially in relatively mild cases of heart failure.

A less invasive measure is definitely needed. To develop a less invasive method for modifying autonomic balance, we have examined the effect of Zusanli electrical stimulation. This method has been used to treat various diseases in oriental medicine.

To ensure these effects of traditional medicine, we have conducted animal experiments. The results have shown depressor and sympathetic neuroinhibitory (static) effect during Zusanli electrical stimulation. These effects are mediated by the changes in neural arc. We have also demonstrated that dynamic characteristics of baroreflex neural and peripheral arcs did not change by Zusanli electrical stimulation. We conclude that application of electrical acupuncture can suppress sympathetic nerve activity but does not affect the dynamic characteristics of the arterial baroreflex system, indicating no deleterious effect on orthostatic tolerance.

References

[1] M. Li, C. Zheng, T. Sato, T. Kawada, M. Sugimachi, K. Sunagawa. "Vagal nerve stimulation markedly improves long-term survival after chronic heart failure in rats." *Circulation.* Vol. 109, pp. 120-124, Jan. 2004.

[2] T. Sato, T. Kawada, M. Inagaki, T. Shishido, H. Takaki, M. Sugimachi, K. Sunagawa, "New analytic framework for understanding sympathetic baroreflex control of arterial pressure." *Am. J. Physiol. Heart Circ Physiol.* vol. 276, no. 6, pp. H2251-H2261, Jun. 1999.

[3] P. Z. Marmarelis and V. Z. Marmarelis, Analysis of Physiological Systems: The White-Noise Approach, New York, NY: Plenum, 1978.

[4] J. S. Bendat, and A. G. Piersol, Random Data: Analysis & Measurement Procedures, 3rd Ed., New York, NY: Wiley-Interscience, 2000.

[5] D. Michikami, A. Kamiya, T. Kawada, M. Inagaki, T. Shishido, K. Yamamoto, H. Ariumi, S. Iwase, J. Sugenoya, K. Sunagawa, M. Sugimachi. "Short-term electroacupuncture at Zusanli resets the arterial baroreflex neural arc toward lower sympathetic nerve activity." *Am J Physiol Heart Circ Physiol.* vol. 291, pp. H318-H326, Jul. 2006.

Autonomic Neuroscience: Basic and Clinical 144 (2008) 43–49

Contents lists available at ScienceDirect

Autonomic Neuroscience: Basic and Clinical

journal homepage: www.elsevier.com/locate/autneu

Electroacupuncture changes the relationship between cardiac and renal sympathetic nerve activities in anesthetized cats

Hiromi Yamamoto [a,*], Toru Kawada [b], Atsunori Kamiya [b], Toru Kita [a], Masaru Sugimachi [b]

[a] Department of Cardiovascular Medicine, Graduate School of Medicine, Kyoto University, Kyoto 606-8501, Japan
[b] Department of Cardiovascular Dynamics, Advanced Medical Engineering Center, National Cardiovascular Center Research Institute, Osaka 565-8565, Japan

ARTICLE INFO

Article history:
Received 5 June 2008
Received in revised form 13 August 2008
Accepted 12 September 2008

Keywords:
Hind limb stimulation
Baroreflex
Arterial blood pressure
Heart rate

ABSTRACT

Electroacupuncture (EA) is known to affect hemodynamics through modulation of efferent sympathetic nerve activity (SNA), however, possible regional differences in the SNA response to EA remains to be examined. Based on the discordance between arterial blood pressure and heart rate changes during EA, we hypothesized that regional differences would occur among SNAs during EA. To test this hypothesis, we compared changes in cardiac and renal SNAs in response to 1-min EA (10 Hz or 2 Hz) of a hind limb in adult cats anesthetized with pentobarbital sodium. Renal SNA remained decreased for 1 min during EA ($P<0.01$ for both 10 Hz and 2 Hz). In contrast, cardiac SNA tented to decrease only in the beginning of EA. It increased during the end of EA ($P<0.05$ for 2 Hz) and further increased after the end of EA ($P<0.01$ both for 10 Hz and 2 Hz). There was a quasi-linear relationship between renal and cardiac SNAs with a slope of 0.69 (i.e., renal SNA was more suppressed than cardiac SNA) during the last 10 s of EA. The discrepancy between the renal and cardiac SNAs persisted after sinoaortic denervation and vagotomy. In conclusion, EA evokes differential patterns of SNA responses and changes the relationship between cardiac and renal SNAs.

1. Introduction

Electroacupuncture stimulation has been used to modulate autonomic nervous activity and cardiovascular function (Kimura and Sato, 1997; Lin et al., 2001). Several studies have demonstrated that arterial blood pressure (AP) is decreased by acupuncture-like stimulation in anesthetized animals (Kline et al., 1978; Ku and Zou, 1993; Lee and Kim, 1994; Zhou et al., 2005). The cardiovascular responses induced by acupuncture-like stimulation are reflexes mediated via somatic afferent nerves and autonomic efferent nerves (Sato et al., 1994, 2002). Although slow-onset, long-lasting effects may be characteristics of acupuncture, rapid-onset, short-lasting effects are also reported in some experimental conditions. In anesthetized rats, Ohsawa et al. (1995) reported that acupuncture-like stimulation of a hind limb decreased AP in association with a decrease in renal sympathetic nerve activity (RSNA). Uchida et al. (2007) reported that acupuncture-like stimulation of a hind limb induced decreases in cardiac sympathetic nerve activity (CSNA) and heart rate (HR). On the other hand, Kobayashi et al. (1998) reported that acupuncture stimulation produced variable responses including tachycardia, bradycardia, or no responses. We hypothesized that regional differences in sympathetic nerve activities would account for the diverse HR response and more consistent hypotensive response reported during EA. Although Sato et al. (1981) reported that stimulation of group III muscle afferent fibers of a hind limb induces either bradycardic or tachycardic response in anesthetized cats, they did not measure efferent sympathetic nerve activities. To test the hypothesis that EA would evoke regional differences among sympathetic efferent nerve activities, we simultaneously recorded and directly compared CSNA and RSNA during EA in anesthetized cats. The kidneys are important for a long-term AP control via the maintenance of sodium and water balance (DiBona, 2005). At the same time, because the kidneys receive approximately 20% of the cardiac output in resting humans (Rowell, 1974), we thought changes in RSNA could contribute to the acute AP control. We first examined changes in AP, HR, CSNA, and RSNA in response to 10-Hz or 2-Hz EA of a hind limb. We then investigated possible roles of arterial baroreflex and vagal nerve activities in the effects of EA using sinoaortic denervation and vagotomy.

2. Methods

2.1. Surgical preparation

Animal care was provided in strict accordance with the Guiding Principles for the Care and Use of Animals in the Field of Physiological Sciences approved by the Physiological Society of Japan. All protocols were approved by the Animal Subject Committee of National Cardiovascular Center. Adult cats weighing 3.0 to 5.2 kg were anesthetized by an intraperitoneal injection of pentobarbital sodium (30–35 mg/kg) and ventilated mechanically via a tracheal tube with oxygen-supplied room air. The depth of anesthesia was maintained with a continuous intravenous infusion of pentobarbital sodium (1–2 $mg \cdot kg^{-1} \cdot h^{-1}$) through a catheter inserted into the right femoral vein. Vecuronium bromide (0.5–

* Corresponding author. Tel.: +81 75 751 3195; fax: +81 75 751 3203.
E-mail address: hiromi@kuhp.kyoto-u.ac.jp (H. Yamamoto).

1566-0702/$ – see front matter © 2008 Elsevier B.V. All rights reserved.
doi:10.1016/j.autneu.2008.09.002

1.0 mg·kg^{-1}·h^{-1}, i.v.) was given continuously to suppress muscular activity. AP was measured using a catheter-tip manometer inserted from the right femoral artery and advanced into the thoracic aorta. A pair of bipolar stainless steel wire electrodes (AS633, Cooner Wire, Chatsworth, CA) was attached to a branch of the left renal nerve through a flank incision. The nerve fibers peripheral to the electrodes were tightly ligated and crushed to remove afferent signals from the kidney. The nerve fibers and the electrodes were secured with silicone glue (Kwik-Sil, World Precision Instruments, Sarasota, FL). Another pair of bipolar stainless steel wire electrodes was attached to a branch of the left cardiac sympathetic nerve arising from the left stellate ganglion through a resection of the left second rib. The nerve fibers distal to the electrodes were sectioned to eliminate afferent signals from the heart. The nerve fibers and the electrodes were secured with silicone glue. Because the influence of the right cardiac sympathetic nerve on sinus rhythm is greater than that of he left cardiac sympathetic nerve (Yasunaga and Nosaka, 1979), we kept the right cardiac sympathetic nerve intact to preserve the HR response to EA. One rationale for recording left CSNA was that there was no significant laterality in left and right CSNAs during sympathetic perturbation via the arterial baroreflex (Kawada et al., 2003). The preamplified nerve activity signals were band-pass-filtered between 150 and 1000 Hz and then rectified and low-pass-filtered with a cut-off frequency of 30 Hz to quantify CSNA and RSNA. For sinoaortic denervation and vagotomy, we sectioned all nerves surrounding the common carotid arteries at the neck. The carotid sinus nerves were crushed by tight ligatures of 3-0 silk suture around tissues between the internal and external carotid arteries.

2.2. Electroacupuncture

In the supine position, both hind limbs were lifted to obtain a better view of the lateral sides of the lower legs. An EA needle with a diameter of 0.2 mm (CE0123, Seirin-Kasei, Japan) was inserted into a point below the knee joint just lateral to the tibia to the depth of approximately 10 mm. Another EA needle was inserted into the skin behind the ankle as the ground. EA was applied to either the left or right leg using an isolator connected to an electrical stimulator (SEN 7203, Nihon Kohden, Japan). The pulse width was set at 500 μs and the stimulus frequency was set at either 10 or 2 Hz. The stimulus current was set in the range from 2 to 5 mA (2.9 ± 1.1 mA, mean ± SD) to produce an AP decrease of more than 5 mmHg at 10-Hz stimulation.

2.3. Protocols

Protocol 1. To examine regional differences in sympathetic nerve activities, we applied 10-Hz or 2-Hz EA for 1 min while measuring AP, HR, CSNA, and RSNA. EA was applied to either the left or right hind limb in random order. An interval of at least 5 min was allowed between the EA trials.

Protocol 2. We applied 10-Hz electrical stimulation to a nonspecific control point in the front of the right thigh to examine whether changes in AP, HR, CSNA, and RSNA observed in Protocol 1 were caused by nonspecific responses to the electrical stimulation.

Protocol 3. To examine possible roles of arterial baroreflex and vagal nerve activities in the effects of EA, we performed sinoaortic denervation and vagotomy. Approximately 20 min after the sinoaortic denervation and vagotomy, changes in AP, HR, CSNA, and RSNA in response to 10-Hz EA were examined.

Protocol 4. To confirm baroreflex-induced changes in sympathetic nerve activity, changes in CSNA and RSNA in response to an intravenous phenylephrine injection (5 μg/kg) were examined before performing sinoaortic denervation and vagotomy. CSNA and

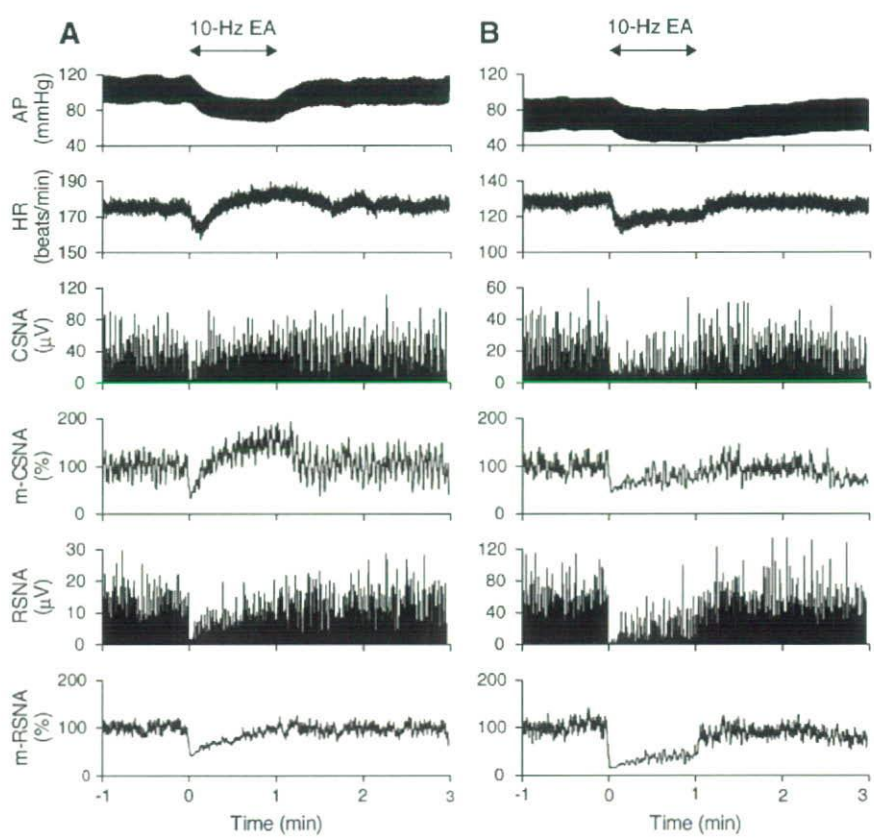

Fig. 1. Time series of arterial pressure (AP), heart rate (HR), cardiac sympathetic nerve activity (CSNA), 2-s moving averaged CSNA (m-CSNA), renal sympathetic nerve activity (RSNA), and 2-s moving averaged RSNA (m-RSNA) during 10-Hz electroacupuncture (EA) obtained from two different animals (see main text for details).

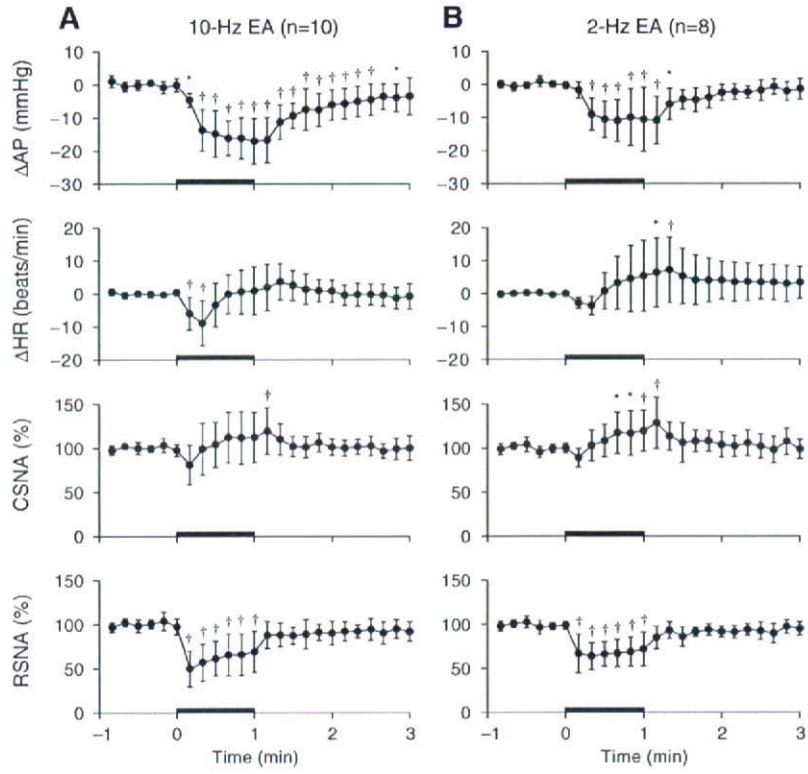

Fig. 2. Changes in arterial pressure (ΔAP), changes in heart rate (ΔHR), percent values of cardiac sympathetic nerve activity (CSNA), and percent values of renal sympathetic nerve activity (RSNA) during 10-Hz electroacupuncture (EA) (A) and 2-Hz EA (B) averaged for all trials. Values are the mean±SD. *$P<0.05$ and †$P<0.01$ from the first data point during the pre-EA baseline period.

RSNA were expected to be decreased by phenylephrine-induced hypertension.

2.4. Data analysis

Data were digitized by a 16-bit analog-to-digital converter (Contec, Japan) and stored at 200 Hz in a dedicated laboratory computer system. Because the absolute voltage of nerve activity varied among animals depending on the recording conditions, we normalized the nerve activity by a 1-min averaged value during the baseline condition before applying stimulation. The minimal inter-burst activity of the nerve signal was treated as the zero level. To examine changes in AP, HR, CSNA, and RSNA, we used 10-s averaged data. The data were analyzed using repeated-measures one-way analysis of variance (ANOVA) followed by Dunnett's test (Glantz, 2002). The first data point of the baseline condition was treated as the control. To analyze the correlation between changes in AP and CSNA or RSNA, that between changes in AP and changes in HR, and that between CSNA and RSNA, we performed a linear regression analysis between the two variables (Glantz, 2002). To analyze the correlation between changes in HR and CSNA or RSNA, we first fit the relationship to the following equation using a nonlinear least square fitting (a downhill simplex method) (Nelder and Mead, 1965).

$$y = \text{slope} \times \log_{10}(\text{offset} + x) + \text{intercept}$$

where x and y represent changes in HR and sympathetic nerve activity, respectively. After determining the optimal offset value for x, an ordinary linear regression analysis was performed between [$\log_{10}$(offset+x)] and y to examine the significance of the slope. In all of the regression analyses, the correlation was considered significant when the slope was significantly different from zero. We used paired-t test to examine the difference between the CSNA and RSNA during the time period of maximum AP elevation induced by phenylephrine in Protocol 4. To examine the difference in the initial HR response to 10-Hz EA between Protocols 1 and 3, we used unpaired-t test because the number of trials was different between Protocols 1 and 3. The differences were considered significant at $P<0.05$.

3. Results

Typical recordings of 10-Hz EA obtained from two different cats are shown in Fig. 1. Horizontal arrows above the top panels indicate the period of EA. In one animal (Fig. 1A), AP was decreased by EA. HR decreased initially but increased from approximately 20 s after the onset of EA. As can be seen in the 2-s moving averaged signal (m-CSNA), CSNA exhibited changes similar to HR, i.e., it decreased at the onset of EA but gradually increased above the baseline level during the later portion of 1-min EA. RSNA and its 2-s moving averaged signal (m-RSNA) decreased at the onset of EA and gradually returned toward the baseline level. In another animal (Fig. 1B), both AP and HR were decreased by EA. Both CSNA and RSNA were also suppressed during EA, but the magnitude of suppression was greater in RSNA than in CSNA. Among the 5 animals, three showed the former type of AP and HR responses and remaining two showed the latter type. The type of AP and HR responses was consistent in each animal, i.e., the observed difference depended on the animal rather than the trial.

Fig. 2A summarizes changes in AP, HR, CSNA, and RSNA in response to 10-Hz EA. We performed EA trials in the left and right hind limbs in each animal and pooled data for 10 trials from 5 animals because there did not appear to be significant laterality in the effects of EA. The thick line on the abscissa in each panel indicates the period of EA. Baseline AP and HR values were 101 ± 17 mmHg and 161 ± 24 beats/min, respectively. AP was significantly decreased by EA and the decrease lasted over 1 min after